

© Copyright 2017

Qi Lee

Incorporating an otolith-derived environmental index into growth for stock
assessment models

Qi Lee

A thesis

submitted in partial fulfillment of the
requirements for the degree of

Master of Science

University of Washington

2017

Committee:

André E. Punt, Chair

Timothy E. Essington

James T. Thorson

Vladlena V. Gertseva

Program Authorized to Offer Degree:

Aquatic and Fishery Sciences

University of Washington

Abstract

Incorporating an otolith-derived environmental index into growth for stock assessment models

Qi Lee

Chair of the Supervisory Committee:
Dr. André E. Punt, Professor & Director
Aquatic and Fishery Sciences

Growth is one of the key demographic processes for population dynamics. There is a growing body of literature showing that growth in fish is plastic over time, and affected by climate variability. However, time-varying indices of growth variation are not often incorporated into stock assessment models, on which fishery management advice is based, and growth is often estimated with time-invariant parameters or incorporating annual variation without an explicit growth model. This is due to a lack of a general framework for deciding when and whether to incorporate indices of time-varying individual growth into an assessment model, and of a general understanding of its mechanistic drivers. In this thesis, I developed a framework to evaluate the suitability of incorporating a time-varying growth index into a stock assessment model, and use risk

analysis to evaluate its management-related advantages and shortcomings. I then developed a nonlinear mixed-effects model that estimates a time-varying growth index from otolith increment data, while also allowing for random individual effects. Including an accurate time-varying growth index generally is expected to improve estimates of spawning stock biomass and recruitment in a stock assessment, while a relatively small number of otoliths is required to attain such a level of accuracy when estimating the random year effects. The simulation framework described in this thesis can be applied across multiple stocks, to further our understanding of the effects of modelling time-varying growth on population dynamics.

TABLE OF CONTENTS

CONTENTS

Chapter 1 Introduction	1
Chapter 2 The benefits and risks of incorporating climate-driven growth variation into stock assessment models, with application to Splitnose Rockfish (<i>Sebastes diploproa</i>)	4
Abstract.....	4
Introduction.....	5
Materials and Methods.....	7
Overview.....	7
Incorporating climate indices of individual growth into assessment models	8
Biological Characteristics	9
Simulation Method.....	10
Results.....	15
Estimation performance	16
Sensitivity to high β values	19
Management implications	19
Discussion.....	21
Supplementary Materials	25
Tables	26
Figures	31

Chapter 3 Extracting a time-varying climate-driven growth index for use in stock assessment	
models	38
Abstract	38
Introduction	38
Methods	42
Model description	42
Estimation method	44
Fits to data	44
Simulation study	44
Operating model	45
Scenarios	46
Sensitivity analyses	47
Performance metrics	47
Results	48
Simulation-testing	48
Sensitivity to error	50
Comparison to the index from Black (2009)	51
Discussion	52
Tables	57
Figures	60

LIST OF FIGURES

Figure 2.1 Flowchart depicting the general steps of the simulation process.....	31
Figure 2.2 Time series of relative errors in estimates of spawning stock biomass for scenarios with the correctly-specified index data (i.e. OM-0-A and OM-1-B).32	32
Figure 2.3 Time series of relative errors in estimates of recruitment for scenarios with the correctly-specified environmental index data (i.e. OM-0-A and OM-1-B)....	34
Figure 2.4 Time series of relative errors in estimates of spawning stock biomass (top row) and recruitment (bottom row) showing the effects of varying the observation model.	36
Figure 2.5 Time series of relative errors in estimates of spawning stock biomass (top row) and recruitment (bottom row) showing the results of the sensitivity analysis to the accuracy of the index.	37
Figure 3.1 Example increment growth curves for each life history, and the corresponding year effects.....	60
Figure 3.2 Summary of results from the scenarios where there was no year effect.	61
Figure 3.3 Summary of results from the sensitivity analysis of year effect estimates to sample size, for a minimum age limit of 0.3 of the maximum age.	63
Figure 3.4 Summary of results from the sensitivity analysis to minimum age limit at a sample size of 20, the lowest sample size tested.....	65
Figure 3.5 Summary of results from the sensitivity analysis to the value of σ_{inc} .	66
Figure 3.6 Summary of results from the sensitivity analysis to the values for σ_w and σ_K	67
Figure 3.7 Summary of results from the sensitivity analysis to the values for β_w and β_K , at a sample size of 100.....	68
Figure 3.8 Summary of results of setting for β_w and β_K to the stock assessment values, where the signs are inversed.....	69
Figure 3.9 Model fits to actual otolith increment data for 6 individual splitnose rockfish, selected out of the total sample size of 66.	70

Figure 3.10 Difference (absolute error) between estimated year effects from fitting the proposed model to the actual otolith data, compared with the published index from Black (2009). 71

LIST OF TABLES

Table 2.1 Summary of OMs, and their associated values.....	26
Table 2.2 Data types and error structures used in data generation (Gertseva et al., 2009).	27
Table 2.3 Summary of scenarios tested.....	28
Table 2.4 MAREs for the model parameters and derived quantities.....	29
Table 2.5 Table summary of all scenarios tested.	30
Table 3.1 Description of the parameters used in the model.	57
Table 3.2 Description of life histories used and their associated parameters.	57
Table 3.3 Description of uniform distributions used to generate data.....	58
Table 3.4 Values used in sensitivity analyses	59
Table 3.5 Fixed effect estimates and AICc values for each model configuration fit to the actual data splitnose rockfish.	59

ACKNOWLEDGEMENTS

A world of gratitude goes out to my advisor, André Punt, for all the guidance, advice, and encouragement he provided me these last three years. I literally could not have done this without him.

A huge thank you also goes out to Jim Thorson for his incredibly helpful comments and ideas on how to improve my work, my self, and my way of thinking through problems.

I would also like to thank the other members of my committee – Tim Essington and Vlada Gertseva – for their help and perspectives on this project.

I am indebted to the past and current members of the Punt lab – Kelli F. Johnson, Felipe Hurtado Ferro, Chantel R. Wetzel, Caitlin I. Allen Akselrud, Lee Cronin-Fine, and Kristin Privitera-Johnson – for coding tips, shared commiseration, and moral support.

Thank you also to Melissa Haltuch, James Hastie, Ian Taylor, and countless others at the NOAA Northwest Fisheries Science Centre for comments, patient answers to ignorant questions, and constant encouragement.

This work was funded by the National Oceanic and Atmospheric Administration (NOAA) Fisheries and the Environment (FATE) programme, project 13-01.

DEDICATION

To my parents

To my mentors – past, present, and future –

Thank you for everything.

CHAPTER 1 INTRODUCTION

In fisheries science, an important challenge is to understand and predict a population dynamics system that has a seemingly infinite number of components and interactions, e.g. growth, recruitment, environment, mortality, fishing pressure, etc. This is achieved using stock assessment methods. Integrated single species stock assessment models combine a variety of data sources in a single analysis, maximizing a joint likelihood function to obtain parameter estimates that best describe the species' population dynamics (Fournier and Archibald, 1982; Maunder and Punt, 2013). These estimates are then used to set management targets, to allow for sustainable use of the resource (Punt, 2008). One of the main challenges for stock assessment scientists is to strike a balance between optimizing model complexity and reducing uncertainty to optimize model structure, in order to achieve a “sweet spot” known in ecology as the Medawar zone (Grimm et al., 2005). The best way to structure a stock assessment is still a topic under debate, with scientists prioritizing different aspects (e.g. growth - Lorenzen, 2016; maturity - Palumbi, 2004; recruitment - Thorson et al., 2013). Furthermore, many fisheries managers are moving towards ecosystem-based fisheries management (EBFM), where the fishery is evaluated in the context of the ecosystem, which would also include interactions with other species, the environment, the marine habitat, etc. (Pikitch et al., 2004). The challenge faced with these increasingly complex systems is that there is limited information on the mechanistic drivers behind variation in vital rates of fish stocks.

Most parameters are estimated as temporally- and spatially-invariant in traditional stock assessments. However, understanding variability in life history characteristics in space and time further helps determine the most appropriate assessment model structure as well as address uncertainty in assessment results (Gertseva et al., 2010). With ocean temperatures projected to increase (Kirtman et al., 2013), species distribution (Pinsky et al., 2013; Thorson et al., 2016), behaviors (Biro et al., 2010; Dale et al., 2016), and abundance (Mueter et al., 2011; Schirripa and

Colbert, 2006) are expected to adapt and respond accordingly, resulting in the demand for management strategies that are robust to such changes (A'mar et al., 2009; Holt and Punt, 2009; Ianelli et al., 2011). Stock assessments need to be able to accommodate the inclusion of climate variables accordingly, but without adding too many parameters.

Individual growth is an integral component of population dynamics models (Francis, 2016). As with most other components of a stock assessment, the parameters of the growth model are often pre-specified, or estimated as constants, despite evidence that individual growth varies across time, age, and cohorts (Lorenzen, 2016; Stawitz et al., 2015; Thorson and Minte-Vera, 2016). Unfortunately, population dynamics models tend to perform poorly when growth is inaccurately approximated (Helser and Brodziak, 1998), because time-varying growth has the potential to affect spawning potential of a stock (Brander, 2007). Thorson and Minte-Vera (2016) found that the best models with a single time-varying effect could explain on average 50% of variability in weight-at-age data for exploited stocks, with year effects explaining approximately 45% of variability. Including variables such as those year effects in a stock assessment model could more accurately describe the dynamics of fish populations and potentially disentangle whether fluctuations in a fish population are due to time-varying environmental conditions or fishing. Given an increased understanding of the role of climate in population dynamics (Brander, 2010), resource managers may be better equipped to evaluate management alternatives (Basson, 1999; Tolimieri and Levin, 2005). However, there is little guidance available for when to incorporate year effects on growth in the stock assessments used as the basis for advice to managers to support fisheries decision making. Furthermore, long-term time series of growth deviations may be difficult to obtain without confounding with other parameters such as selectivity (Stawitz et al., 2015).

Otoliths, or “ear stones”, are calcified structures found in the heads of bony fish, used for balance and/or hearing (Campana, 1999), to which increments are added annually. As such, they record information on their growth and environment at different temporal scales, allowing for

individual growth trajectories to be observed (Campana, 1990). Black et al. (2005) detrended otolith increment data for a species of rockfish with a method called dendrochronology. The residuals were averaged to form a dimensionless index, that also correlated with several climate indices as well as indices from other species in the region. In this thesis, a decision framework for incorporating a similar time-varying growth index is developed and tested using simulation. Additionally, a fishery-independent method for deriving growth indices from otolith data – dendrochronology – is expanded on, and a novel model developed to estimate both year and individual effects, and simulation-tested to gain insight on its effective sample size. In doing so, an overall framework for extracting a time-varying index and the conditions under which it would be suitable for inclusion in a stock assessment is shown in this thesis. The results of these analyses will help stock assessment scientists decide how to structure their stock assessments to include time-varying growth, and take us a step closer towards achieving the Medawar Zone.

CHAPTER 2 THE BENEFITS AND RISKS OF INCORPORATING CLIMATE-DRIVEN GROWTH VARIATION INTO STOCK ASSESSMENT MODELS, WITH APPLICATION TO SPLITNOSE ROCKFISH (*SEBASTES DIPLOPROA*)

ABSTRACT

Indices of annual growth variation are not routinely incorporated into fisheries stock assessment models, due to a lack of a general framework for deciding when to include these indices, and of a mechanistic understanding about growth drivers. Such incorporation may also not necessarily lead to improved estimation or management performance. We develop a way to incorporate such an index into an assessment model (Stock Synthesis), and use risk analysis to evaluate its management-related advantages and shortcomings. We applied this method to splitnose rockfish (*Sebastes diploproa*), where a previously-developed growth index is highly correlated with decadal-scale climate indices. We find that including a similar index in the simulated assessment increases precision and reduces bias of parameter estimates. However, not including an index or including a completely erroneous index led to highly imprecise estimates when growth was strongly climate-driven. Including this growth index when individual growth was actually constant did not lead to poorer estimation performance. The risk analysis approach can be applied to other stocks to evaluate the consequences of including time-varying growth indices.

INTRODUCTION

Climate and environmental factors can have a large impact on population and community dynamics (Harley et al., 2006; Pinsky et al., 2013; Rowe and Terry, 2014). One of the ways in which the environment can play a major role in determining the dynamics of fish populations is through the metabolism, and ultimately growth, of individual fish (Ait Youcef et al., 2015; Sünksen et al., 2010). However, little guidance is available for whether or when to incorporate environmentally-driven growth variables into the stock assessments used as the basis for advice to managers to support fisheries decision making. Such inclusion could more accurately describe the dynamics of fish populations, and potentially disentangle whether fluctuations in biomass are due to time-varying environmental conditions or fishing.

Much of our current understanding of how to best incorporate environmental information into stock assessments derives from recruitment-environment relationships (e.g., Mueter et al., 2011; Schirripa et al., 2009; Thorson et al., 2013), as opposed to individual fish growth. Individual growth is an integral component of fisheries stock assessment, and the relationship between age and size is often estimated in assessments (Taylor and Methot, 2013), based on the assumption that the parameters of this relationship are constant over space and time (Lorenzen, 2016). However, it has been shown (e.g., Stawitz et al., 2015; Weatherley, 1990; Webber and Thorson, 2016) that growth in fish is inherently plastic, and that this “constant growth” paradigm needs to be challenged (Lorenzen, 2016; Thorson and Minte-Vera, 2016). Defining climate-growth relationships would allow fishery managers to better discriminate the effects of climate

from those of fishing, and make more accurate predictions of future stock size, should there be a means of projecting the relationship into the future (Black et al., 2008).

Black (2009) examined ring widths of rockfish otoliths and reduced these widths to species-specific dimensionless indices that are correlated with similar dendrochronology indices from geoducks and trees in the same general area. These indices were also found to coincide with climate indices in the California Current System. However, these growth indices have never been incorporated in assessments due, *inter alia*, to the lack of a general framework for deciding whether and under what circumstances to do so.

Many studies have used simulation to evaluate the benefits of incorporating indices of climate on recruitment in assessments, notably Schirripa et al. (2009) for sablefish, Hulson et al. (2013) and A'mar et al. (2009) for walleye pollock, and Haltuch and Punt (2011) for groundfish generally. Simulations are used to evaluate model performance and test the effects of different hypotheses on management outcomes (e.g., Johnson et al., 2014). However, this has yet to be done for time-varying growth. Maunder and Watters (2003) proposed a general framework for integrating environmental time series in assessments, where simulations are used to test and compare a model that includes environmental effects with the traditional approach where environment variables are ignored. Maunder and Watters (2003) focused on the ability to correctly identify the relationship between a selected variable in the model and the environmental variable, and to accurately estimate specific parameters, and not on the impact of these relationships on management outcomes.

The goal of this study is to propose and illustrate a risk-analysis approach to estimating the benefits and risks of incorporating a climate index on somatic fish growth

into stock assessments. Our analyses are conditioned closely upon a climate index developed by Black (2009) and the stock assessment for splitnose rockfish (*Sebastes diploproa*) in the Northeast Pacific Ocean (Gertseva et al., 2009), and evaluate management outcomes associated with various climate-growth scenarios. We expand on Maunder and Watters (2003) and develop a table using simulation modeling to provide guidance on whether incorporation of climate information is justified in a given case.

MATERIALS AND METHODS

Overview

The risk-analysis was developed using a widely-used stock assessment platform – Stock Synthesis (SS; Methot and Wetzel, 2013). SS can incorporate all available data into a single analysis, and estimate parameters by maximizing the product of the likelihood function for each data type Fournier and Archibald, “A General Theory for Analyzing Catch at Age Data”; Maunder and Punt, “A Review of Integrated Analysis in Fisheries Stock Assessment.”. The assessment was simplified to ensure that results are widely applicable to other contexts. The numbers of fishing fleets and surveys were reduced to one of each data type. Operating models (OMs) were used to describe “true” population dynamics and quantity of data for five states of nature – one with constant growth, and four with time-varying environmentally-driven growth indices that vary in terms of auto-correlation and relationship to the OM growth parameters. Each simulation was projected for fifty years using the OM (with the relevant assumptions made for each OM, i.e. constant future growth for one and time-varying future growth for the other four), with fishing occurring under a constant-catch limit obtained from the OM. Implementation

error was not simulated, so catch was assumed to be taken exactly. The OM outputs based in the historical and forecast periods were considered “true” for the simulations.

Observation models simulated the data-gathering process. A total of 1,100 data sets were generated, with 100 data sets for each combination of OM and observation model. Each data set was analyzed using two estimation methods (EMs). We examined the performance of two EMs - one that estimated time-invariant growth, and one that assumed growth was correlated with an available environmental index. Management reference points were estimated using these EMs, and used to set a catch limit that was projected forward as a constant in the simulated fishery system (as represented in the OM). The resultant forecasted outcomes were then compared with the “true” (i.e. OM) quantities to obtain performance metrics, such as lost yield and final stock biomass. A summary of the overall process can be found in Figure 2.1.

Incorporating climate indices of individual growth into assessment models

As the growth model most commonly used in stock assessments (Essington et al., 2001; Francis, 2016), this study is based, for simplicity, on the von Bertalanffy growth function (Von Bertalanffy, 1957):

$$L_t = L_\infty(1 - e^{-K(t-t_0)}) \quad (1)$$

where L_t is the length of the fish at time t , L_∞ is the asymptotic length of the fish and a ratio of anabolic to catabolic factors, K is the intrinsic growth rate and a catabolic factor, and t_0 is a constant that adjusts the model along a time axis. Temperature is known to affect catabolism, and thus both K and L_∞ (Brunel and Dickey-Collas, 2010; Lorenzen, 2016), with Kimura (2008) showing a negative correlation between the two parameters.

Temporal variation in growth due to changes in environmental drivers can be incorporated in an assessment by modifying the values of the parameters of the growth function. In SS, an environmental index can be linked to the values of the growth parameters in two ways – additively or multiplicatively (Methot and Wetzel, 2013). In this study, we included an annual index ε_t that is associated with variation in growth, using a multiplicative relationship (Eq. 2) for both maximum size for sex s :

$$L_{\infty,s,t} = L_{\infty,s,base} \cdot e^{\beta_{L,s}\varepsilon_t} \quad (2a)$$

and growth rate:

$$K_{s,t} = K_{s,base} \cdot e^{\beta_{K,s}\varepsilon_t} \quad (2b)$$

where β is the parameter linking the growth parameter to the environmental index, $L_{\infty,s,base}$ and $K_{s,base}$ are median values for the asymptotic length and growth rate parameters for sex s , and length-at-age in each year is then calculated from length-at-age the previous year (using Eq. 1). Should the index value be sufficiently large to result in a negative growth increment (e.g. if $L_{\infty,t} < L_t$ from Eq. 1), the individuals remain at the same size for the following year and are assumed to not experience any growth, which thus avoids the occurrence of “shrinking” fish.

Biological Characteristics

Populations were simulated based on parameters obtained from a simplified version of the assessment (Supplementary Table S1; Gertseva et al., 2009). The data sets with the longest time series for a single fishing fleet and a single fishery-independent survey were selected (Supplementary Figure S2.1c). In the assessment approved for management (Gertseva et al., 2009), the parameters governing natural mortality (M) and

steepness (h) were pre-specified, while log initial recruitment ($\ln R_0$) and individual-growth parameters including length at age 0 (L_0), L_∞ , K , and variability in size-at-age for fish less than L_0 (CV_0) and for fish up to L_∞ (CV_∞) were estimated. Growth of splitnose rockfish is sex-specific, with males estimated to grow at a faster rate (i.e. higher K_{male}), while females are estimated to attain larger sizes (i.e. higher $L_{\infty, female}$). This is also one of the two rockfish species for which a climate-growth index was developed by Black (2009).

Simulation Method

Index data generation

The environmental index ε_t was simulated using an autoregressive (AR) model with bias correction (Eq. 3), adapted from Thorson et al. (2014), with parameters calculated for splitnose rockfish. The environmental index was unique to each replicate within each state of nature, and scaled to a mean of 0.

$$\varepsilon_t = \begin{cases} \rho_{splitnose} \varepsilon_{t-1} + \sqrt{1 - \rho_{splitnose}^2} \omega_t & \text{for } t > 1 \\ \omega_t & \text{for } t = 1 \end{cases}$$

$$\omega_t \sim \text{Normal} \left(\frac{-\sigma_{splitnose}^2}{2} \times \frac{1 - \rho_{splitnose}}{\sqrt{1 - \rho_{splitnose}^2}}, \sigma_{splitnose}^2 \right) \quad (3)$$

where ω_t is independent and identically normally distributed variation for year t . As the index is treated as data, the species-specific parameters in Eq. 3 ($\rho_{splitnose}$ and $\sigma_{splitnose}^2$) were defined external to the OM, and fixed. Comparative runs (across OMs) used the same sequence of random numbers.

Five trends in growth were investigated, based on the extent of auto-correlation (i.e. $\rho_{splitnose}$) in the environmental indices and the strength of the relationship between

the environmental index and the growth parameters (i.e. $\beta_{L,S}$ and $\beta_{K,S}$; Eq. 2; Table 2.1). Sensitivity analyses were conducted for a series of β and $\rho_{splitnose}$ values in the OM, using OM 2 (weakly climate-driven growth) as the base case. As the values for β increase, so too does the impact of the environmental index (and vice-versa). The series of β values tested ranged from 0 to 0.5, in 0.1 increments. The higher the value of $\rho_{splitnose}$, the more that long periods of time have a series of fast or slow growth, should the index be highly correlated with growth. We tested scenarios with indices of varying levels of auto-correlation, ranging the $\rho_{splitnose}$ values from 0.0 (i.e. white noise) to 0.8 by 0.2 increments, and a final maximum high value of 0.95.

The values for β for OMs 2 and 3 were estimated by including the otolith index data as an index on the growth parameters, and applying the assessment to these data. The values for β for OMs 4 and 5 were fixed at a high value of 0.3, as determined by the sensitivity analysis, with positive values for K and negative values for L_{∞} , consistent with the notion of having opposite effects. $\rho_{splitnose}$ and $\sigma_{splitnose}^2$ in OMs 2 and 4 were determined by fitting an AR-1 model to the otolith index obtained from Black (pers. comm.). As such, the environmental index in OM 2 had the most realistic characteristics, while OMs 3-5 were exploratory.

Observation errors

Observation error was added to the expected values for each data type in the OMs to generate data sets for use in the EMs (Table 2.2). Additional variability for each simulation was included in the form of independent and lognormally-distributed yearly deviations about a Beverton-Holt stock-recruitment relationship (Methot and Wetzel,

2013). A bias-correction factor (Methot and Taylor, 2011) was applied in the EM to avoid bias in estimation of expected recruitment when there is less data.

Four observations of the environmental index were explored to examine the effects of including an incorrectly-observed index:

- i. 158 years of environmental indices (108 historical, 50 projected) observed without error; i.e., the index used to generate the data
- ii. 158 years of an independent time series of random errors (white noise), generated under $N(0,1)$
- iii. 20 years of historical environmental indices observed without error, with 50 years of projected indices, i.e. a shortened time series of data when there is insufficient historical information
- iv. 158 years of auto-correlated indices generated using the same model and values for ρ_p and σ_p^2 as the “true” index, but with a different starting seed, i.e. a time series of auto-correlated indices that seems plausible but is completely inaccurate

These scenarios were similar to those described by Stawitz et al. (2015), where growth anomaly patterns were estimated to be in one of three predominant forms – trendless, sustained trend, and near-zero. Sensitivity of the EM to the accuracy of the environmental index was also examined, using OM 5 as a base. This was done by creating a second auto-correlated index ($\varepsilon_{t,wrong}$) using the same AR parameters and process (Eq. 3), and adding it to the true index ($\varepsilon_{t,true}$) in varying proportions a , which ranged from 1 to 0 at 0.2 increments, to create a new index ($\varepsilon_{t,new}$):

$$\varepsilon_{t,new} = \sqrt{a} \cdot \varepsilon_{t,true} + \sqrt{(1-a)} \cdot \varepsilon_{t,wrong} \quad (4)$$

This procedure therefore leads to a new environmental index for which $a \cdot 100\%$ of the variance is correct, and $(1 - a) \cdot 100\%$ of the variance is auto-correlated noise (i.e., the correlation between $\varepsilon_{t,true}$ and $\varepsilon_{t,new}$ is \sqrt{a}). The new index $\varepsilon_{t,wrong}$ is calculated to have the same variance and first-order autocorrelation as the true index.

Estimation methods

The estimation scenarios mimicked an actual assessment process, by estimating model parameters and management reference points. Supplementary Table S1 lists the key parameters of the population dynamics model and how they are estimated in the EM. Two EMs were used – one where the index was included (β is estimated), and one where the index was not ($\beta = 0$). Each combination of OM, observation model, and EM is referred to as a scenario, and 16 scenarios were evaluated (Table 2.3).

Performance evaluation

Performance was evaluated for each scenario by (a) comparing spawning stock biomass (SSB), recruitment, and parameters from the OM with corresponding estimates from the EM, and (b) conducting forecasts of the OM in which future catches are based on management reference points estimated by the EM and summarizing the results of the projections in terms of “lost yield” and differences between ideal and anticipated stock status when management is based on the EM. Each of these components is discussed below.

The estimation performance of the EMs was summarized using relative errors by year for SSB and recruitment, using $RE = (\hat{\theta} - \theta)/\theta$, and median absolute relative errors (MARE = $\text{median}(|(\hat{\theta} - \theta)/\theta|)$) for other parameter estimates (e.g. growth, R_o) and derived quantities (e.g. maximum sustainable yield MSY, virgin stock biomass B_o , final

year biomass B_{2008}). These median values were used as a measure of bias, as occasional outliers greatly skewed the mean values. MAREs have been used previously as a measure of precision for point parameter estimates (e.g. Johnson et al., 2014).

The management implications of growth variability and how it is handled in the assessment were evaluated by assuming that management aims to follow a constant catch strategy, based on MSY , and implemented without error. This harvest strategy was selected for illustrative purposes. MSY is calculated from the base growth, the stock-recruit, and the selectivity parameters (Methot and Wetzel, 2013), as found in the first year of the simulation, and unaffected by any time-varying biology. The simulated fishery system is projected forward using this constant-catch strategy, and the consequences evaluated using selected metrics. Projecting with the MSY obtained from the OM represents the “true” state of the resource for that replicate, with all relevant hypotheses associated with that OM. Recruitment in the OM during the forecast period is simulated given recruitment variation, while management performance during the forecast period is calculated by simulating future population sizes and catches given either that future growth is constant (for OM 1) or time-varying (for OMs 2-5).

The EM was also used to estimate MSY , which was then used as the basis for projections for each year of a 50-year forecast period. These “estimated” catches were provided to the OM and a second set of projections undertaken in which the catches taken from the population in the OM were set to the “estimated” catches. Thus, the OM was projected forward twice, once using the MSY from the OM (“true yield”) and once using the estimates of MSY from EM (“projected yield”).

The risk for each EM given the true state of nature was calculated in terms of relative lost yield, the forecasted final year stock status, and the proportion of replicates

overfished (see below). With the exception of the final metric (proportion overfished), all the metrics were calculated for each simulation replicate, and the median value and interquartile range across replicates (representing central tendency and precision, respectively) reported.

- **Relative Lost Yield:** Difference between estimated retained catch (yield from the EM) and true retained catch (yield from the OM) for the first projected year as a proportion of true catch $((\text{projected yield} - \text{true yield}) / \text{true yield})$
- **Final Stock Status:** Ratio of projected (using MSY from EM) final spawning stock biomass to true (using MSY from OM) final stock biomass $(\text{projected } B_{2058} / \text{true } B_{2058})$
- **Proportion Overfished:** Proportion of replicates where the final biomass is less than 0.25 of B_0 , which is the metric by which the stock would be declared overfished $\{\text{Gertseva et al., 2009; number of } [(\text{projected } B_{2058} / \text{true } B_0) < 0.25] / \text{number of runs}\}$. The final year is used in this metric as it would be near-impossible for a fishery to recover from an overfished state under a constant-catch harvest strategy without any intervention.

RESULTS

The simplified base model (Supplementary Figure S2.1c) had catch start in 1902, peaking in 1998 (Supplementary Figure S2.1a). Overall SSB increased when the environmental index was added, and the peaks and troughs in the time series appeared more pronounced (Supplementary Figure S2.1b).

Several replicates (10/1100) failed to converge (non-positive definite Hessian matrix), and were discarded. If a replicate failed within a single scenario, the results for

that replicate for all scenarios were discarded. In a true assessment, model configurations could be manually adjusted to ensure convergence, but such methods would not be feasible in a simulation study so we instead discarded these few replicates.

Estimation performance

Time-invariant growth in OM

The two EMs – one correctly specified (1-0-A), one over-parameterized (1-0-B) – performed well when growth was constant in the OM. There was a slight overall positive bias (measured in median RE) for SSB and recruitment for both EMs, although the median RE for each time series was less than 7%. Over-parameterization did not result in a substantial difference in the bias of SSB and recruitment because the assessment model generally estimated link parameters (β) close to zero (Figs. 2.2a(i) and 2.4a(i)). Base growth parameters were also estimated without bias and precisely, and were similar for the two EMs (Table 2.4).

Correctly specifying environmental index in EM

Most of the correctly-specified scenarios (2-1-B, 3-1-B, 4-1-B, 5-1-B; Figs. 2.2b-e(ii), 2.4a(ii), 2.4b(ii)) were able to estimate SSB and recruitment accurately and precisely when growth was time-varying in the OM, with a similar bias to those from the scenarios with constant growth and either correct or over-parameterized models (Table 2.4). The only exception was when β was set to a higher value and growth was highly-varying (OM 4; Fig. 2.2d), which greatly decreased precision, even if the median SSB and recruitment estimates across simulations were fairly unbiased (median relative error <13% for all years).

Misspecifying the time-varying index

We examined two ways in which the environmental index used in the EM differed from the true index driving the population dynamics.

The EM assumed that growth was constant up until the time series began in scenarios where the EM only had 20 out of the 108 years of the environmental data (observation model 2; scenarios 2-2-B and 5-2-B). Base growth parameters (K and L_∞) tended to be under-estimated (Supplementary Table S2.2: rows 5 and 14) for these scenarios. These errors increased when growth parameters varied more over time (comparing OM 5 to OM 2). SSB was generally biased over time in these cases, with both positive and negative bias during portions of the time series. Median RE was positive at the start of the time series and became negative in the later years, and only tended to zero during the last few years of the time series, when growth was weakly climate-driven with the correct model and a shortened index (Fig. 2.4a(iii)). Precision was similar to that of the correctly-specified model for both SSB and recruitment (Fig. 2.4a(ii)). Comparatively, precision of the SSB and recruitment estimates was much poorer for the scenario with strongly climate-driven growth and the shortened index data (Fig. 2.4b(iii)) than when growth was weakly climate-driven. SSB was over-estimated (up to 50% for some years) for this OM, although the median REs became closer to zero when the environmental data started.

In the sensitivity analysis using partially-correct indices (Eq. 4), bias in SSB and recruitment estimates remained relatively small when the index was correctly-specified compared to being correctly-specified up to 80% ($a = 0.8$), although precision decreased as the value of a decreased (Figs. 2.5(ii-iii)). Thereafter, as a decreased, estimates of SSB became increasingly biased (again, both positively and negatively) and less precise than

the model with a correct index (Figs. 2.5(iv-vi)), although bias in estimates of recruitment remained relatively small until the index was completely misspecified ($a = 0$; Fig. 2.5(vii)), where the estimates of SSB became highly negatively biased in the later years.

Completely misspecifying the environmental index, either as an equally auto-correlated index or as random white noise (observation models 3 and 4), did not affect the estimation of the base growth parameters, SSB, and recruitment estimations when growth was weakly climate-driven (OM 2; Figs. 2.4a(iv) and 2.4a(v)). However, precision and accuracy of these estimates greatly decreased when growth was strongly climate-driven (OM 5; Figs. 2.4b(iv) and 2.4b(v)). The point estimates of the base growth parameters in those scenarios were biased by $>10\%$ under when the index was wrong and growth was misspecified (Table 2.4).

Model misspecification (not allowing for time-varying growth)

Not allowing for time-varying growth resulted in imprecise and biased estimates of SSB (Figs. 2b-e(i)), although recruitment was estimated precisely and without bias (Figs. 3b-e(i)). Growth parameters were biased, with K being negatively biased, and L_∞ positively biased. The magnitude of bias in SSB and recruitment also increased with increasing β values (compare Figs. 2.2b(i) and 2.3b(i) with Figs. 2.2d(i) and 2.3d(i)). There was a large bias in the estimates of SSB and recruitment when the EM was misspecified (Figs. 2.2d and 2.3d), although the level of precision appears to be similar irrespective of whether the model was correctly specified or not. Misspecified EMs under OMs with high β values were the only scenarios where estimates of recruitment were biased (Fig. 3d(i)). Precision of SSB and recruitment also decreased in scenarios when

autocorrelation within the environmental index increased and growth was assumed constant in the EM (Fig. 2.2c(i), 2.3c(i) and Supplementary Figure S2.3).

Sensitivity to high β values

The magnitude of bias (in terms of median relative error) in the estimates of SSB and recruitment increased with the value for β when growth was assumed constant in the EM (Supplementary Figure S2.2). The pattern of bias (positive in the early years, and decreasing to become negative in the later years) remained the same across scenarios. Supplementary Figure S2 also shows that precision (measured using the inter-quantile range) of SSB and recruitment decreased as β was increased, regardless of whether allowance was made for time-varying growth in the EM. The problems in estimation found for high β values were probably caused by issues in the process of generating data. The high variance in growth caused fish to attain large sizes at young ages, and remain at that size during years where the index was at lower values, resulting in higher average sizes-at-age, as can be seen in Supplementary Table S2.3.

Management implications

Table 2.5 summarizes the implications of managing under a constant catch strategy, based on an estimate of MSY from monitoring data collected from the fishery and perhaps based on a misspecified assessment model. Median lost yield varied across scenarios, while median final stock status was similar, although inter-simulation variability differed. The proportion overfished differed across OMs, but was similar between EMs.

The proportions of replicates that resulted in overfished populations ranged from 0.28 to 0.51 across the scenarios (Table 2.5). Some of the randomly generated recruitment deviations resulted in populations with extreme spawning stock biomass levels, both high and low, with low levels causing populations to crash. Low stock sizes might have contributed to the relatively high proportion of replicates being considered overfished, as shown by the 0.45 value from scenario 1-0-A, when the assessment was correctly specified and growth was time-invariant.

Most EMs tended to provide MSY estimates that were median-unbiased, given the correct index data, regardless of whether time-varying growth was accounted for. However, inter-simulation variability (measured in terms of inter-quantile range), increased greatly when the EM was misspecified, i.e. growth was assumed to be constant (2-0-A, 3-0-A, 5-0-A). The exception to both these results was the OM 4, where β was set to a high level. In that case, there were negligible differences in MSY estimates between the misspecified EM with time-invariant growth and the correctly-specified EM (Table 2.5, scenarios 4-O-A and 4-O-B).

The estimates of MSY were positively biased when the EM was based on an incorrect environmental index (scenarios 2-3-B, 2-4-B, 5-3-B, 5-4-B). This resulted in up to a median of 24% of yield being lost in the OM where growth is strongly climate-driven (OM 5; Table 2.5). Inter-simulation variability was very high for the scenarios based on OM 5, while this was not the case for the scenarios where growth was weakly climate-driven (OM 2). Supplementary Table S2.4 shows an increase in inter-simulation variability of management quantities as the accuracy of the index decreased, although bias remained the same across scenarios.

Model misspecification (i.e. assuming time-invariant growth when growth was actually varying over time) resulted in more biased and less precise estimates of MSY (Table 2.4), resulting in a larger median and wider range of lost yield across replicates respectively (Table 2.5). Table 5 also shows that the inter-quantile range of lost yield (i.e. the imprecision of MSY estimates) decreased when the EM was correctly specified, particularly when growth varied over time (e.g., comparing 3-0-A vs. 3-0-B).

DISCUSSION

Incorporating accurate growth indices resulted in higher precision and less bias in parameter estimates and management outcomes. These effects are more pronounced if the environmental index was highly auto-correlated and/or had high variance. The degree of bias and inaccuracies are largely defined by the variance of the time-varying index, and the strength of its auto-correlation. The risks of obtaining inaccurate or imprecise abundance estimates associated with including an inaccurate index with low variance seem on par with not including an index at all when growth was either weakly time-varying or constant. On the other hand, including an inaccurate index ($a < 0.6$) or not including one at all when growth strongly correlated with an index of high variance resulted in highly biased and inaccurate estimates of stock size. Estimating time-varying growth when the growth index is correct results in the most precise and least biased estimates. Including an inaccurate index risks similar biases and precision in derived quantities as not including an index at all, although parameter estimates were slightly more accurate when growth is weakly time-varying. Allowing for time-varying growth in the form of an index does not risk significant degradation in estimation performance even when growth is not actually time-varying, although this scenario is unlikely (e.g., Stawitz

et al., 2015; Thorson and Minte-Vera, 2016). Therefore, inclusion of the index would likely improve the performance of the model, regardless of how accurate the index is, if the growth index under consideration is weakly auto-correlated and weakly linked to the growth parameters.

Based on the results for OM 2, the most “realistic” OM, and the properties of the growth index developed in Black (2009), we would recommend consideration of including this index in the assessment of splitnose rockfish. If a climate-driven growth index were to be considered for use in an assessment, we would recommend fitting an AR-1 model to the index, using these parameters to generate new simulated growth indices, and simulation-testing their inclusion in the stock assessment model. The results were obtained from only one set of life history parameters, but the simulation-based risk analysis approach could be conditioned on the data and biology of other stocks to illustrate whether to include a growth index for a different specific stock assessment.

A growth index for which 60% of the variance is correct ($a = 0.6$) could still lead to estimates of parameters and derived quantities that have similar bias and precision as not including the index at all, when growth is strongly time-varying (OM 5). This case study suggests that environmental indices should only be used when there is high confidence in their accuracy. For example, Thorson and Minte-Vera “Relative Magnitude of Cohort, Age, and Year Effects on Size at Age of Exploited Marine Fishes.” found that the best models with a single time-varying effect could explain on average 50% of variability in weight-at-age for exploited stocks, with year-effects (i.e., annual indices like those explored here) explaining approximately 45% of variability. Stawitz et al. (2015) described a state-space model that was fit to fishery-dependent and -independent data for 29 stocks of Pacific groundfish, and found that approximately 40% of the modeled stocks exhibited

time-varying growth. Whereas it is highly unlikely that it is possible to observe the true underlying mechanism by which growth varies over time and generate an exact environmental index, it may be feasible to identify an environmental index that has a 0.77 ($\sqrt{a} = 0.60$) correlation with true variation in growth. This could be feasible by estimating similarities in growth variation among species (Stawitz et al., 2015). Additionally, Maunder & Watters (2003) recommend an integrated approach with additional process error when including an environmental time series into stock assessment models. This was not examined here because it is not a standard feature within SS v3.24, used for this research, and should be a subject for future research. However, this approach could presumably be implemented using annual variation in growth, in addition to including the index multiplicatively, and the magnitude of additional variation in growth could be estimated using the Laplace approximation (Thorson et al., 2015a).

Improving the accuracy of growth parameter estimates had a relatively small contribution to total predicted MSY. Furthermore, erroneous parameter and management quantity estimates had negligible impact on future stock size in this case study. This could have been an artifact of having both natural mortality M and steepness h parameters fixed in the assessment. These parameters exhibit a strong influence on reference point estimation, as shown in Mangel et al. (2013), and as such would limit the extent by which growth parameters could affect estimates of MSY. Furthermore, the studied species is long-lived and slow-growing, with a relatively high age of maturity, and a short time series of age data. MSY for long-lived species is expected to have similar sensitivity to changing growth parameters as short-lived species (Thorson et al., 2015b), so we do not expect MSY to be more sensitive to growth variation for short-lived species. Future work should thus consider assessments where there is more data on age and

growth, and/or these parameters are not pre-specified, or based on species where growth may vary more strongly over time (e.g., California Current petrale sole *Eopsetta jordani* or Gulf of Alaska walleye pollock; Stawitz et al., 2015) to more fully determine the effects of incorporating a time-varying index on growth. Alternate forms of time-varying growth such as the sine-wave model or AR models with more lags could also be tested for larger scale effects.

In addition, implementing constant catch exactly (i.e. without error) is unlikely to be the best strategy to use for forecasting the effects of including a time-varying growth index in assessments. The risk analysis approach can be extended to be based on alternative management strategies to perform a full management strategy evaluation (Punt et al., 2016). Conducting an MSE would allow managers to better assess the consequences of including a time-varying growth index in a management strategy that applies harvest control rules (Punt et al., 2016). Punt et al. (2014) summarize studies where this has been done for recruitment.

There has been a recent push to move from single-species towards ecosystem-based fisheries management (EBFM; Pikitch et al., 2004), where environmental factors are taken into consideration to manage the ecosystem as a whole. Therefore, there is a need to further explore various methods for incorporating time-varying growth into assessments that can be also done using other methods as outlined in Thorson and Minte-Vera (2016), or using an ensemble modelling approach (Hollowed et al., 2009). The simulation approach described here can be used as a step towards addressing and incorporating climate effects into somatic growth for a single species. By applying this framework to the splitnose-rockfish-like population, the results in the summary table indicate that modelling time-varying growth in the stock assessment would be

appropriate. More work is needed to test the effects of different indices and other management strategies to fully determine the impacts of incorporating such indices into management.

SUPPLEMENTARY MATERIALS

Supplementary figures and tables can be found in Appendix A.

TABLES

Table 2.1 Summary of OMs, and their associated values.

Number	OM	Strength of Relationship	$\beta_{L,f}$	$\beta_{L,m}$	$\beta_{K,f}$	$\beta_{K,m}$	σ_p^2	Degree of Auto-correlation (ρ_p)
1	Not Climate-Driven	No relationship	0	0	0	0	0.88	Weak (0.33)
2	Weakly Climate-Driven	Weak	-0.12	-	0.13	0.22	0.88	Weak (0.33)
3	Climate-Driven (High AR)	Weak	-0.12	-	0.13	0.22	0.88	Strong (0.95)
4	Climate-Driven (High Beta)	Strong	-0.30	-0.30	0.30	0.30	0.88	Weak (0.33)
5	Climate-Driven (High AR and High Beta)	Strong	-0.30	-0.30	0.30	0.30	0.88	Strong (0.95)

Table 2.2 Data types and error structures used in data generation (Gertseva et al., 2009).

Data Type	Years	Error Distribution	Measure of Uncertainty
Catch – Fishery	1900 - 2008	Lognormal	SE of log(value) = 0.01
Abundance indices – Survey	2003 - 2008	Lognormal	SE of log(value) = 0.25-0.34
Length compositions – Fishery	1978 - 2008	Multinomial	Effective N = 505.4
Length compositions – Fishery (Discard)	1987; 2006 - 2007	Multinomial	Effective N = 505.4
Length compositions – Survey	2003 - 2008	Multinomial	Effective N = 1339
Conditional age-at-length compositions – Survey	2003 - 2008	Multinomial	Effective N = 124.3
Mean body weight – Fishery	2002 - 2008	Lognormal	CV = 0.3
Discards – Fishery	1987; 2002 - 2007	Lognormal	CV = 0.5 (1987); 0.2 (2002-2007)
Environmental index – Black (2009)	1936 - 2006	Known exactly	

Table 2.3 Summary of scenarios tested.

OM	Observation of Env Index	EM	Scenario Label	Scenario Name	
1	Not Climate-Driven	NA	Constant	1-0-A	Constant growth with correct EM
		Wrong	Time-varying	1-0-B	Constant growth with over-parameterized EM
2	Weakly Climate-Driven	NA	Constant	2-0-A	Weakly climate-driven growth with incorrect EM
		Exact	Time-varying	2-1-B	Weakly climate-driven growth with correct EM and index
		Exact (final 20 years only)	Time-varying	2-2-B	Weakly climate-driven growth with correct EM and shortened index
		Wrong (AR-1 model)	Time-varying	2-3-B	Weakly climate-driven growth with correct EM and wrong AR index
		Wrong (white noise)	Time-varying	2-4-B	Weakly climate-driven growth with correct EM and wrong random index
3	Climate-Driven (High AR)	NA	Constant	3-0-A	Highly autocorrelated growth with incorrect EM
		Exact	Time-varying	3-1-B	Highly autocorrelated growth with correct EM and index
4	Climate-Driven (High Beta)	NA	Constant	4-0-A	Highly-varied growth with incorrect EM
		Exact	Time-varying	4-1-B	Highly-varied growth with correct EM and index
5	Climate-Driven (High AR and High Beta)	NA	Constant	5-0-A	Strongly climate-driven growth with incorrect EM
		Exact	Time-varying	5-1-B	Strongly climate-driven growth with correct EM and index
		Exact (final 20 years only)	Time-varying	5-2-B	Strongly climate-driven growth with correct EM and shortened index
		Wrong (AR-1 model)	Time-varying	5-3-B	Strongly climate-driven growth with correct EM and wrong AR index
		Wrong (white noise)	Time-varying	5-4-B	Strongly climate-driven growth with correct EM and wrong random index

Table 2.4 MAREs for the model parameters and derived quantities. The colours go from white to red by order of magnitude, with 0 being white, and larger absolute values being red. The growth parameters in these table are the base parameters of the model, i.e. before the index effects took place. Asterisks (*) denote median absolute (not relative) error as the true values for those parameters are zero.

State of Nature (OM)	Scenario	Parameters												Derived Quantities			
		K_f	K_m	$L_{\infty,f}$	$L_{2,m}$	$\beta_{1,f}$	$\beta_{1,m}$	$\beta_{2,f}$	$\beta_{2,m}$	$CV_{0,f}$	$CV_{0,m}$	$CV_{\infty,f}$	$CV_{\infty,m}$	$\ln R_0$	B_0	B_{2008}	MSY
Not Climate-Driven	1-0-A	0.01	0.01	0.00	0.00	NA	NA	NA	NA	0.02	0.02	0.01	0.01	0.00	0.04	0.12	0.04
	1-0-B	0.01	0.01	0.00	0.00	0.01*	0.01*	0.00*	0.00*	0.02	0.02	0.01	0.01	0.01	0.03	0.12	0.04
Weakly Climate-Driven	2-0-A	0.20	0.19	0.07	0.05	NA	NA	NA	NA	0.03	0.03	0.06	0.05	0.01	0.21	0.15	0.05
	2-1-B	0.03	0.02	0.01	0.01	0.23	0.13	0.09	0.1	0.03	0.02	0.02	0.02	0.01	0.05	0.16	0.04
	2-2-B	0.17	0.16	0.05	0.04	0.91	0.4	0.54	0.49	0.03	0.03	0.06	0.04	0.00	0.2	0.12	0.08
	2-3-B	0.08	0.07	0.03	0.02	1.59	1.11	1.33	1.41	0.03	0.02	0.03	0.02	0.01	0.15	0.18	0.05
	2-4-B	0.11	0.08	0.04	0.02	2.09	1.05	0.71	1.49	0.03	0.02	0.03	0.02	0.01	0.17	0.15	0.06
Climate-Driven (High AR)	3-0-A	0.13	0.14	0.06	0.04	NA	NA	NA	NA	0.04	0.03	0.05	0.04	0.02	0.18	0.23	0.10
	3-1-B	0.02	0.01	0.00	0.00	0.15	0.10	0.04	0.03	0.02	0.02	0.01	0.01	0.00	0.03	0.14	0.04
Climate-Driven (High Beta)	4-0-A	0.51	0.56	0.28	0.31	NA	NA	NA	NA	0.13	0.05	0.23	0.22	0.03	0.61	0.45	0.14
	4-1-B	0.02	0.03	0.01	0.01	0.08	0.09	0.02	0.03	0.03	0.02	0.02	0.02	0.01	0.13	0.21	0.12
Climate-Driven (High AR and High Beta)	5-0-A	0.38	0.44	0.21	0.23	NA	NA	NA	NA	0.10	0.08	0.23	0.23	0.05	0.31	0.59	0.36
	5-1-B	0.02	0.01	0.00	0.00	0.09	0.09	0.01	0.01	0.03	0.02	0.01	0.01	0.01	0.05	0.17	0.05
	5-2-B	0.38	0.43	0.15	0.17	1.44	1.83	0.56	0.58	0.06	0.05	0.13	0.11	0.02	0.56	0.32	0.3
	5-3-B	0.68	0.8	0.43	0.48	1.34	1.41	1.08	1.18	0.12	0.05	0.10	0.07	0.05	1.00	0.59	0.7
	5-4-B	0.25	0.26	0.13	0.15	2.38	2.35	1.27	1.24	0.09	0.07	0.09	0.08	0.06	0.47	0.78	0.49

Table 2.5 Table summary of all scenarios tested.

Scenario Label	Scenario Name	Performance Metric		
		Relative Yield Lost (Interquartile Range)	Est B2058/ True B2058 (Interquartile Range)	Proportion of Replicates Overfished
1-0-A	Constant growth with correct EM	0.0249 (0.0682)	0.955 (0.11)	0.45
1-0-B	Constant growth with over-parameterized EM	0.0254 (0.0687)	0.955 (0.109)	0.45
2-0-A	Weakly climate-driven growth with incorrect EM	0.0666 (0.0859)	0.933 (0.106)	0.31
2-1-B	Weakly climate-driven growth with correct EM and index	0.0436 (0.0634)	0.959 (0.0837)	0.28
2-2-B	Weakly climate-driven growth with correct EM and shortened index	0.0918 (0.0818)	0.912 (0.126)	0.34
2-3-B	Weakly climate-driven growth with correct EM and wrong AR index	0.0633 (0.0919)	0.942 (0.121)	0.32
2-4-B	Weakly climate-driven growth with correct EM and wrong random index	0.0628 (0.0922)	0.93 (0.094)	0.33
3-0-A	Highly autocorrelated growth with incorrect EM	0.0251 (0.192)	0.959 (0.293)	0.43
3-1-B	Highly autocorrelated growth with correct EM and index	0.0329 (0.0574)	0.952 (0.098)	0.47
4-0-A	Highly-varied growth with incorrect EM	0.134 (0.289)	0.95 (0.171)	0.32
4-1-B	Highly-varied growth with correct EM and index	0.131 (0.278)	0.941 (0.216)	0.33
5-0-A	Strongly climate-driven growth with incorrect EM	-0.0308 (0.758)	1.00 (0.555)	0.42
5-1-B	Strongly climate-driven growth with correct EM and index	0.0217 (0.1)	0.985 (0.105)	0.45
5-2-B	Strongly climate-driven growth with correct EM and shortened index	0.237 (0.577)	0.909 (0.681)	0.52
5-3-B	Strongly climate-driven growth with correct EM and wrong AR index	0.206 (1.57)	1.00 (0.844)	0.50
5-4-B	Strongly climate-driven growth with correct EM and wrong random index	-0.097 (1.05)	1.01 (0.631)	0.47

FIGURES

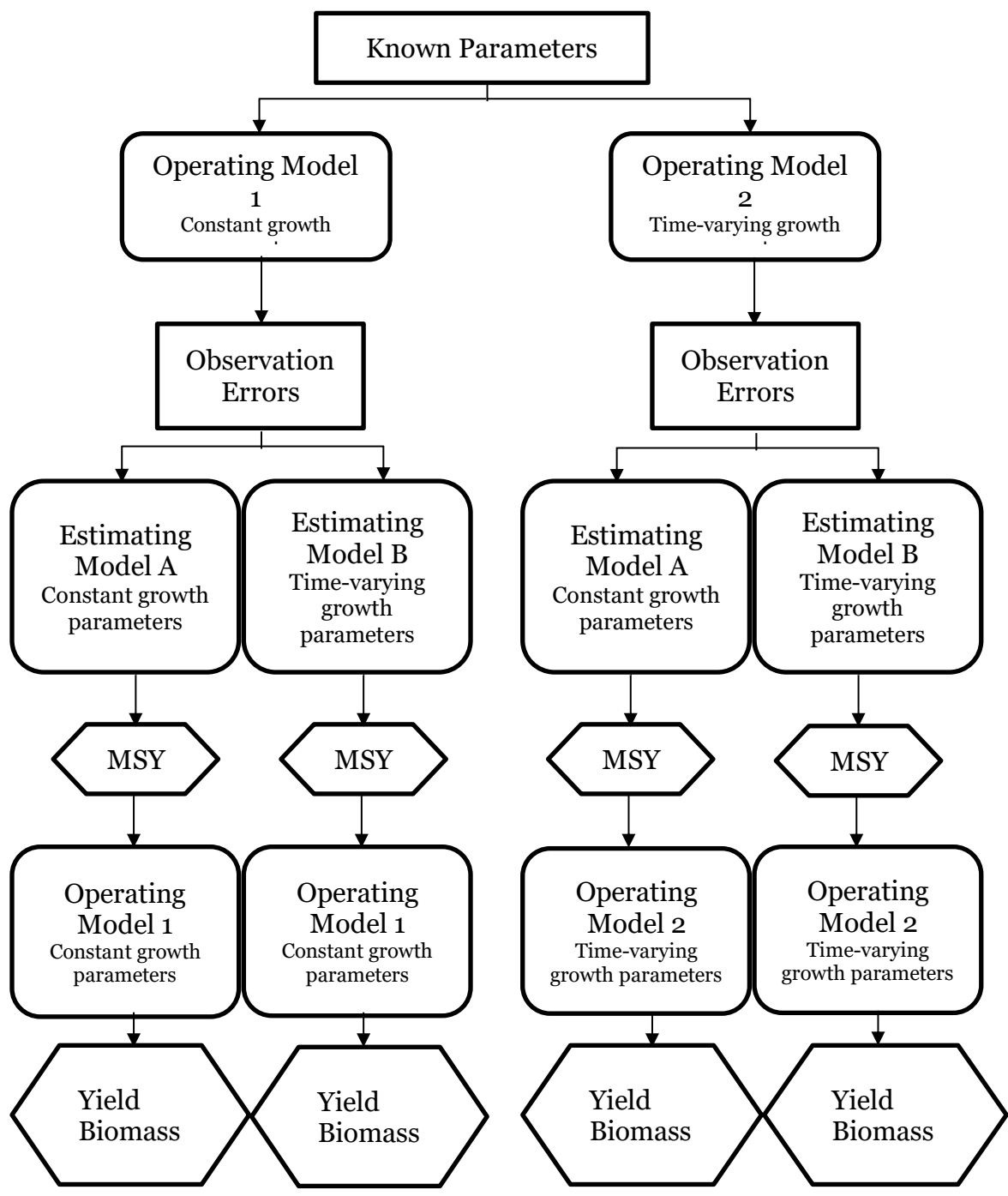


Figure 2.1 Flowchart depicting the general steps of the simulation process. Multiple operating and observation models were considered, but this is not shown here.

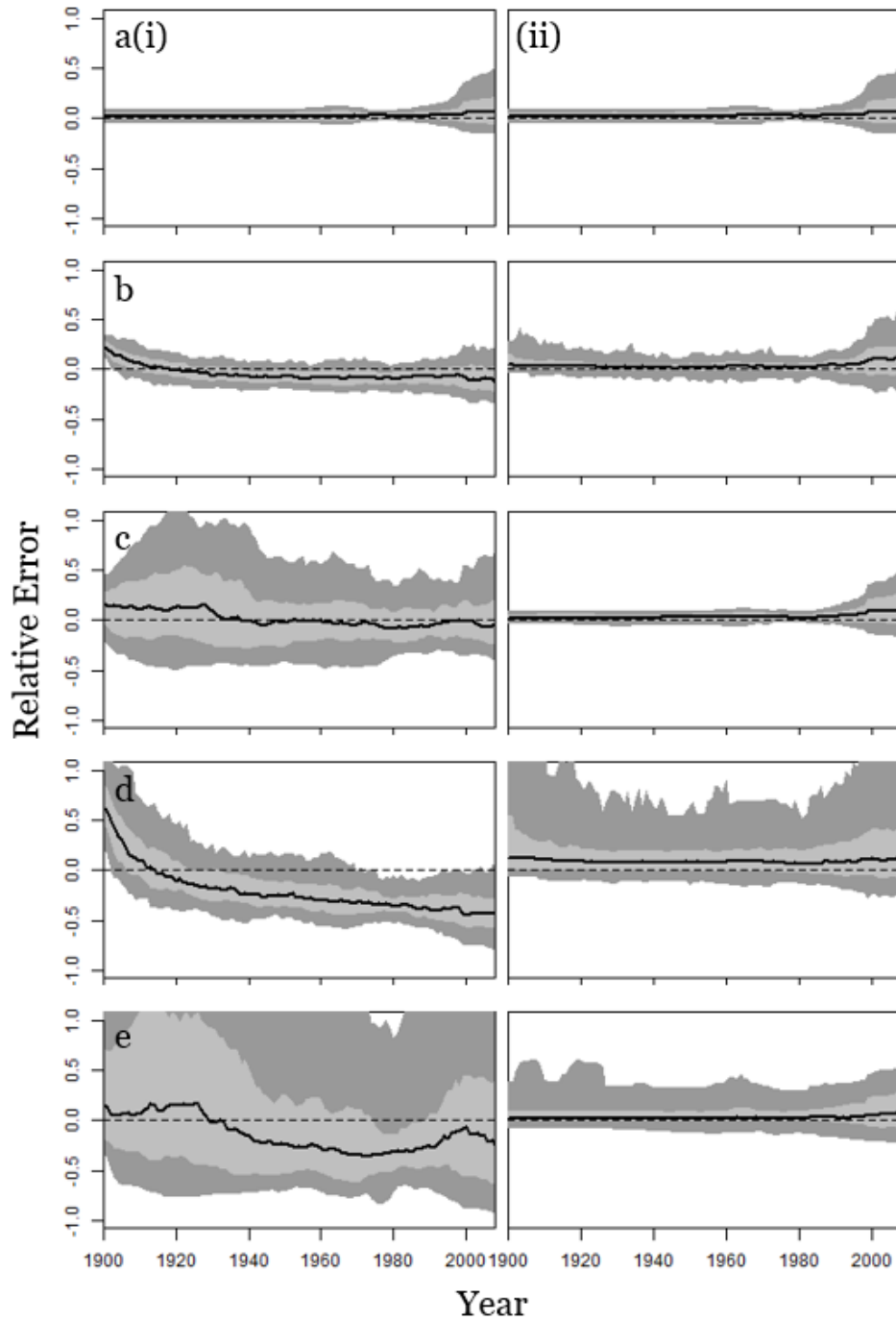


Figure 2.2 Time series of relative errors in estimates of spawning stock biomass for scenarios with the correctly-specified index data (i.e. OM-0-A and OM-1-B). Each row represents a different OM (1-5), and each column represents an EM (A and B). E.g. a(i) corresponds to scenario 1-0-A, a(ii) to 1-1-B, etc. The black line is the median relative

error, the light grey area the 50% simulation intervals, the dark grey area 95% simulation intervals.

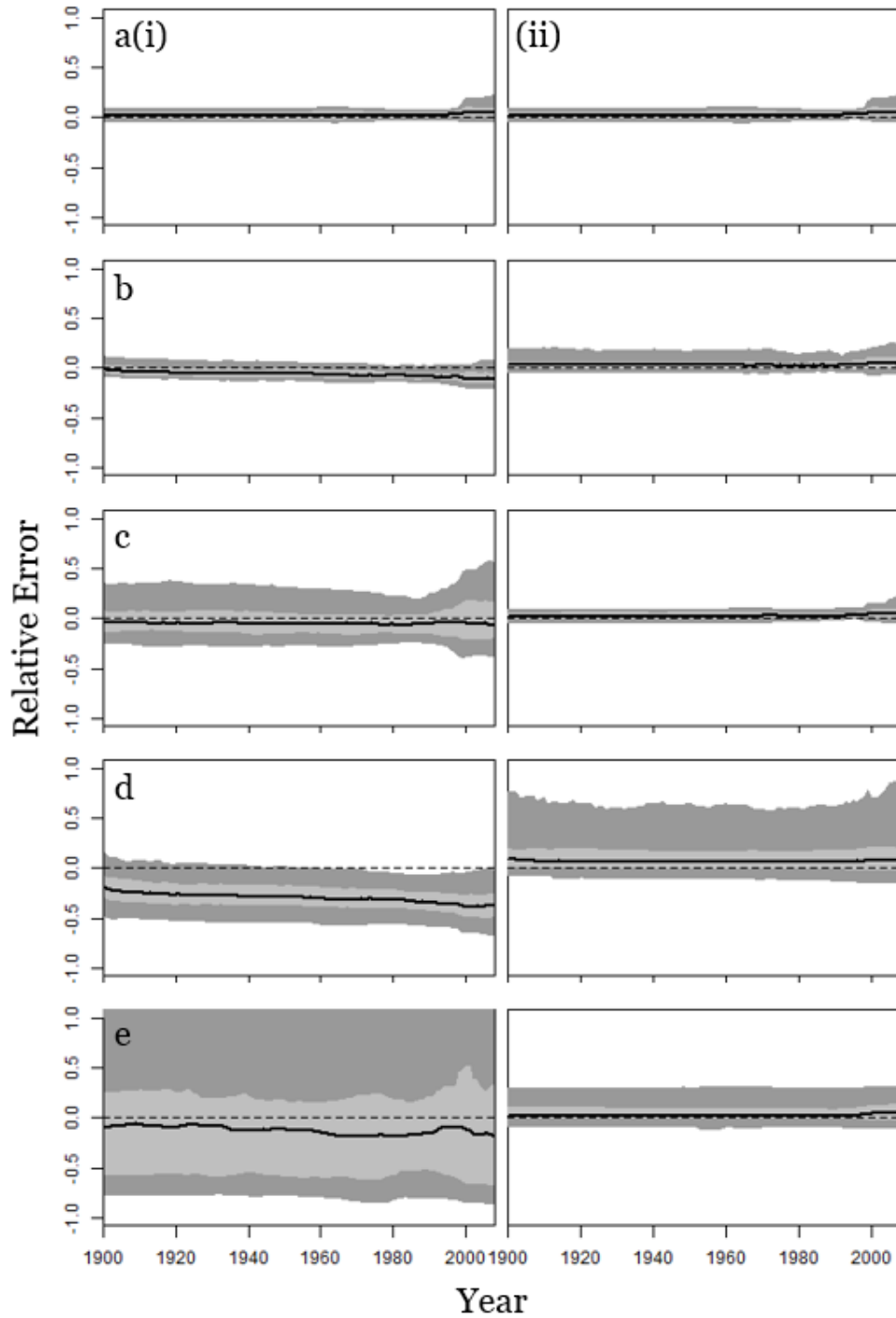


Figure 2.3 Time series of relative errors in estimates of recruitment for scenarios with the correctly-specified environmental index data (i.e. OM-0-A and OM-1-B). Each row represents a different OM (1-5), and each column represents an EM (A and B). E.g. a(i) corresponds to scenario 1-0-A, a(ii) to 1-1-B, etc. The black line is the median relative

error, the light grey area the 50% simulation intervals, the dark grey area 95% simulation intervals.

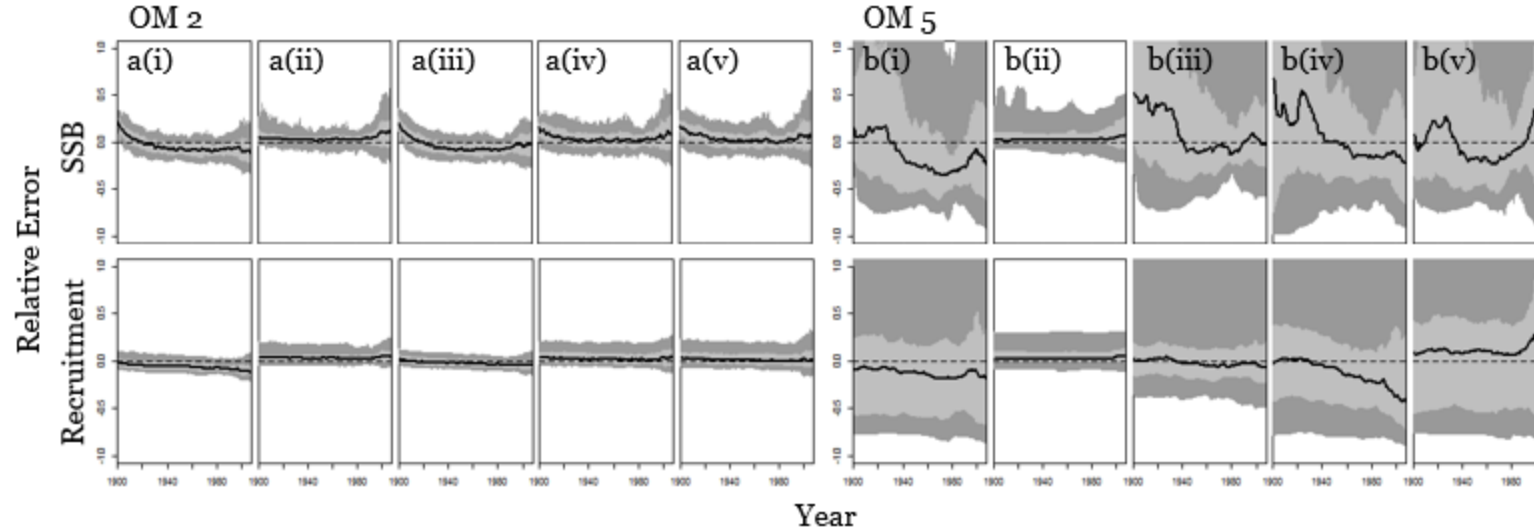


Figure 2.4 Time series of relative errors in estimates of spawning stock biomass (top row) and recruitment (bottom row) showing the effects of varying the observation model. Each column represents a scenario, and the labels correspond to the scenario. Panel a shows results from the weakly climate-driven OM (OM 2), while panel b shows results from the strongly climate-driven OM (OM 5). Labels (i-v) correspond to observations of environmental index 0-4, with their respective EM. E.g. a(i) corresponds to scenario 2-0-A, a(ii) to 2-1-B, a(iii) to 2-2-B, b(i) to 5-0-B etc. The black line is the median relative error, the light grey area the 50% simulation intervals, the dark grey area 95% simulation intervals.

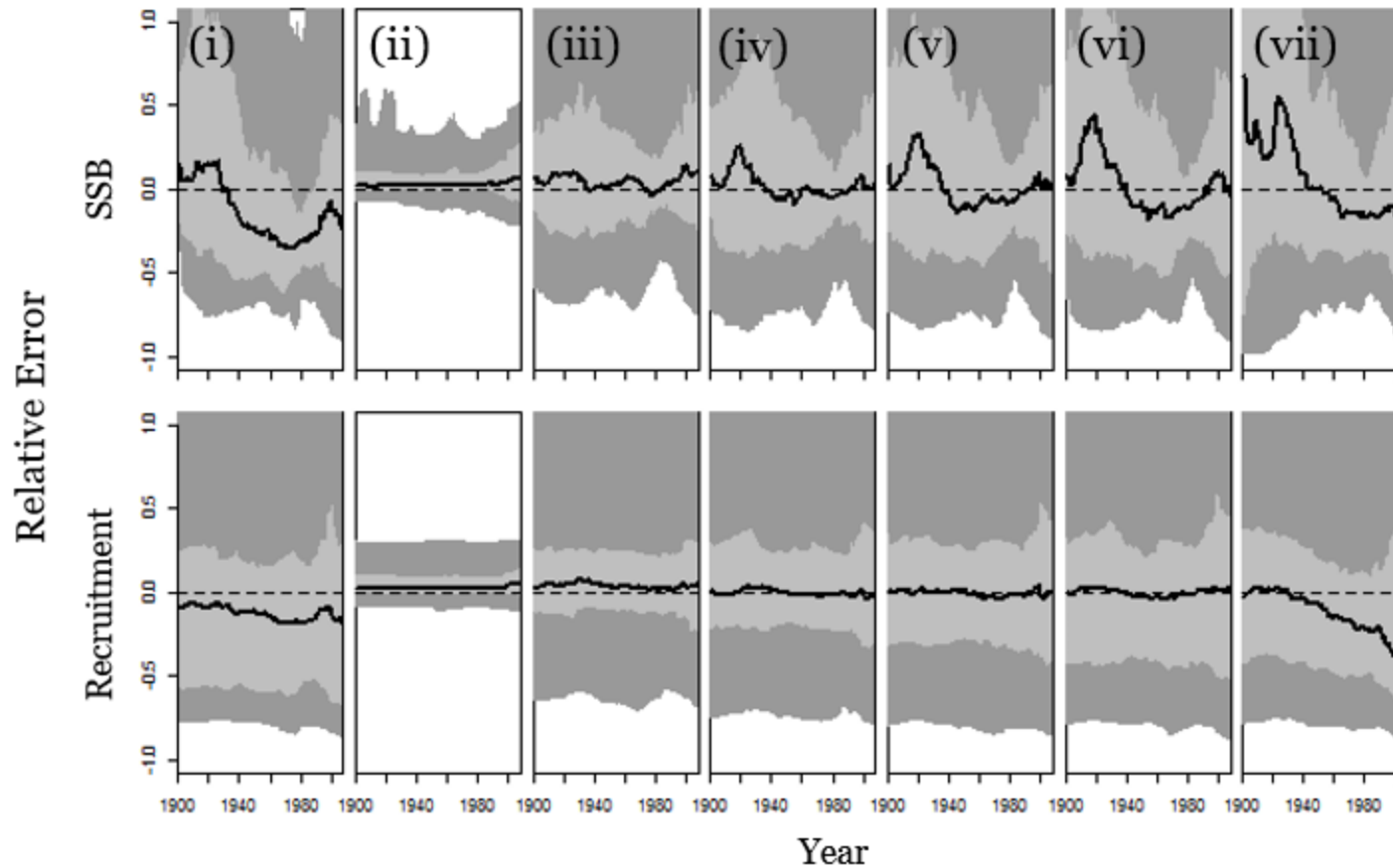


Figure 2.5 Time series of relative errors in estimates of spawning stock biomass (top row) and recruitment (bottom row) showing the results of the sensitivity analysis to the accuracy of the index. Each column represents a scenario, and the labels correspond to the scenario. (i) corresponds to scenario 5-0-A, and (ii-vii) to scenarios where the a value (Eq. 4) goes from 1 to 0, in 0.2 increments ((ii) also corresponds to scenario 5-1-B). The black line is the median relative error, the light grey area the 50% simulation intervals, the dark grey area 95% simulation intervals.

CHAPTER 3 EXTRACTING A TIME-VARYING CLIMATE-DRIVEN GROWTH INDEX FOR USE IN STOCK ASSESSMENT MODELS

ABSTRACT

Understanding the characteristics of individual growth is a critical component of population dynamics. Most fisheries stock assessments assume constant values for each life history parameter, despite growing evidence that growth is plastic at individual, temporal, and spatial scales. Otoliths contain important information pertaining to age and growth, among other things, and otolith increment data correlate with climate indices on a decadal scale. We expand on this concept to include individual-level variation, and developed a nonlinear mixed-effects model to analyze otolith increment data, incorporating both individual- and year-varying random effects. We then fit the model to otolith increment data for splitnose rockfish, and simulation-tested the ability to precisely estimate year effects without bias. Generally, given a sample size of at least 50 otoliths, the model performed well at estimating year effects. With this method, species-specific indices of growth can be extracted from otolith increment data, and potentially be used in stock assessments to detect the effects of climate change on fish growth.

INTRODUCTION

Climate can have varying degrees of impact on a population depending on life history stage, and these impacts are often highly complex and difficult to isolate (Black, 2009). Understanding variability in life history characteristics in space and time further helps determine the most appropriate assessment model structure as well (Gertseva et al., 2010), while time-variation in biological rates adds complexity to the definition of

management targets (Thorson et al., 2015). Estimating the growth of individual fish is important to stock assessment modelling, as growth is one component of the productivity of a stock. Currently, most stock assessments assume time-invariant growth rates (Lorenzen, 2016), even though there is an increasing number of studies that show that growth actually varies over time (e.g. Black, 2009; Stawitz et al., 2015; Thorson and Minte-Vera, 2016), particularly in response to environmental factors such as temperature and food availability (Brett, 1979; Weatherley, 1990).

Collecting long-term (multiple decades) growth data on marine fish populations is often a lengthy and costly process, which makes mechanistic understanding of growth drivers difficult, and indices of growth variation hard to obtain. Stawitz et al. (2015) described a state-space Bayesian modeling approach that uses fishery-dependent and – independent data to detect the presence of growth variation. However, sampling procedures (such as selectivity) could potentially be confounded in the annual growth anomalies, as acknowledged by the authors. Measurement of annually-formed growth increments, using a method known as dendrochronology, has been proposed as an alternative to direct measurements for the reconstruction of time series of environmental variation in growth (Black et al., 2005; Strom et al., 2004; Weisberg, 1993). Dendrochronology may be costly and time-consuming (Stawitz et al., 2015), but would form a fishery-independent source of data as back-calculation would allow for observations for ages that are rarely sampled perhaps due to gear selectivity (Ballagh et al., 2011; López-Abellán et al., 2008). Additionally, otoliths contain historical information about growth that would allow of reconstruction of growth time series potentially dating back to before size-at-age data were available (Begg et al., 2005).

In terrestrial forested ecosystems, tree ring data have been widely used to reconstruct various aspects of climate, disturbance, and community dynamics, and are accepted as a proxy for capturing changes in the environment (e.g. measuring a species' sensitivity to climate). Similarly, bony fish are known to deposit annual rings on their otoliths, much like tree rings (Pannella, 1980). Studies have previously examined the application of dendrochronology techniques to reconstruct time series of ocean conditions (Black, 2009; Strom et al., 2004). Widths between each ring on otoliths of splitnose rockfish (*Sebastes diploproa*) were measured, and detrended using cubic splines and autoregressive models to remove any age-related trends in the data (Black et al., 2005). The resulting time series was averaged to create an environmental index for the species, which was then found to be strongly correlated with various productivity indicators in the California Current Ecosystem and other dendrochronology indices obtained from trees and other marine species in the area (Black, 2009). However, early years of growth data for each otolith – particularly critical in short-lived species (Weisberg et al., 2010) – were removed from the study to allow for better model fit, which could affect the strength of the relationship between growth and the environment, as well as the precision of the resulting indices.

Rather than the use of cubic splines by Black et al. (2005), fish growth is often described with a nonlinear model such as a von Bertalanffy growth curve (Essington et al., 2001; Von Bertalanffy, 1957), although this has not been specifically applied to otolith increment data. Mixed effects models – where fixed effects describe the entire population, and random effects are associated with randomly-selected experimental units within the population (Pinheiro and Bates, 2000) – are often used to describe incremental growth data, repeatedly measured on the same individuals over a period of time ("longitudinal

data", Liang and Zeger, 1986; Zeger and Liang, 1986). This method apparently originated from a study on bacon pigs (Wishart, 1938), and continuing on to emus (Palmer et al., 1991), clams (Escati-Peñaloza et al., 2010), and tree rings (Xu et al., 2014). Weisberg et al. (2010) described additive linear mixed effects models that were empirically used with otolith and increment data for Pacific halibut (*Hippoglossus stenolepis*) and smallmouth bass (*Micropterus dolomieu*) respectively, where year and individual effects were treated as random. A modified von Bertalanffy curve (Von Bertalanffy, 1957) was also fit to the data, although it did not perform well with this parameterization, and only age (and not year or individual) effects were estimated. Furthermore, the models by Weisberg et al. (2010) were not simulation-tested, nor were the year effects cross-validated with other local species, as was done in Black (2009).

The main purpose of this study was to develop a mixed effects model using a von Bertalanffy curve – the most commonly used growth model in stock assessment – that incorporates both random individual effects and random year effects, with the aim of obtaining a time-varying index of growth from otolith increment data. The model was tested on its ability to accurately detect and estimate year effects from simulated otolith increment data, given different samples sizes, life histories, and levels of process and measurement error. To our knowledge, this method (and its parameterization) has not been applied previously for the analysis of otolith band widths for use in estimating climate indices, and has only been made more accessible due to recent developments in nonlinear minimization software.

METHODS

Model description

There are three sources of random variation in the model – the year effects, individual within-fish variation, and process error. Year effects could come from any environmental factor or time-varying factor, while individual effects could potentially come from genetic, environmental or behavioural differences. Process error could come from unknown processes leading to stochasticity and variability in the population dynamics (Rosenberg and Restrepo, 1994). The otolith width (i.e. width of the otolith measured along an axis from the core; w) for individual i at year t was modeled using a von Bertalanffy growth function (Von Bertalanffy, 1957):

$$w_{i,t} = \begin{cases} w_{\infty,i,t} \left(1 - e^{-K_{i,t}(t-t_0)}\right) + \varepsilon_{inc} & \text{for } t = 1 \\ w_{i,t-1} + (1 - e^{-K_{i,t}})(w_{\infty,i,t} - w_{i,t-1}) + \varepsilon_{inc} & \text{for } t > 1 \end{cases}$$

$$\varepsilon_{inc} \sim \text{Normal}(0, \sigma_{inc}) \quad (1a)$$

where w_{∞} is the asymptotic width of the otolith along that axis, K is the intrinsic growth rate, t_0 is the birth year of the fish (essentially $(t - t_0)$ is the age of the fish), ε_{inc} is the process stochasticity, and σ_{inc} is the standard deviation of the process error. t_0 was not estimated within this model because this is not needed to estimate year effects on growth. Eq 1a can also be modified to model otolith growth increments, as opposed to overall widths:

$$w_{i,t} - w_{i,t-1} = (1 - e^{-K_{i,t}})(w_{\infty,i,t} - w_{i,t-1}) + \varepsilon_{inc} \quad \varepsilon_{inc} \sim \text{Normal}(0, \sigma_{inc}) \quad (1b)$$

Environmental factors can sometimes have effects on both w_{∞} and K , often with inverse effects (Brunel and Dickey-Collas, 2010; Kimura, 2008), as there is inherent confounding between growth rate and asymptotic size (Essington et al., 2001; Weisberg et al., 2010).

This confounding stems from the derivation of the parameters in this model, where K is a function of a catabolic factor, and w_∞ is a ratio of anabolic to catabolic factors (as described in Essington et al., 2001; Vincenzi et al., 2016). Normally-distributed random individual effects $\varepsilon_{w_\infty,i}$ and $\varepsilon_{K,i}$ and year effects ε_t were added to the K and w_∞ parameters:

$$\begin{aligned} K_{i,t} &= K_{base} \cdot e^{\varepsilon_{K,i} + \beta_K \cdot \varepsilon_t} & \varepsilon_{K,i} &\sim Normal(0, \sigma_K) \\ w_{\infty,i,t} &= w_{\infty,base} \cdot e^{\varepsilon_{w_\infty,i} + \beta_{w_\infty} \cdot \varepsilon_t} & \varepsilon_{w_\infty,i} &\sim Normal(0, \sigma_w) \\ & & \varepsilon_t &\sim Normal(0,1) \end{aligned} \quad (2)$$

where K_{base} and $w_{\infty,base}$ are the base, mean growth parameters, β_K and β_{w_∞} are parameters linking the growth parameter to the year effects, scaling the year effects accordingly, and σ_K and σ_w are the standard deviations of the individual effects. The year effects are modelled as a single factor identical between the K and w_∞ parameters – a joint model (Warton et al., 2015) that also describes correlation between the two growth parameters over time. They are presumed to be normally-distributed with a mean of 0 for computational convenience such that the model can estimate the mean growth parameters efficiently, with the population generally following an overall mean growth curve. If the combination of individual effect, year effect, and observation error resulted in negative fish growth (i.e. when $w_{i,t,observed}$ was greater than w_∞), that growth increment was resampled at the measurement error level until the increment was positive. If after 50 re-samples, the increment remained negative, it was set to 0.0000001, as otolith growth continues even when fish growth is negligible, due to the physiochemical process involved in otolith growth (Ashworth et al., 2016).

Estimation method

Using Eq. 1b and 2, a nonlinear mixed-effects estimation model was developed to quantify individual and temporal variation in otolith growth increments. This model was implemented using Template Model Builder (TMB; Kristensen et al., 2016). β_K and β_w were freely-estimated, to allow estimation of a positive or negative correlation with the year effects. ε_t was estimated independently (i.e. without an autoregressive component) within this model, with a normal distribution of mean 0 and standard deviation of 1. This was to allow for analyses of the year effects to be done external to this model procedure, such as fitting AR-1 models to them.

Fits to data

Several versions of the estimation method were fit to actual otolith increment data for splitnose rockfish (Black, pers. comm.). These include a model with no individual nor year variation in growth parameters, a model with only individual effects, a model with only year effects, and a model with both year and individual effects. The resultant index of year effects was compared to the published normalized index (Black, 2009; henceforth referred to as the 'published index') using linear regression through the origin.

Simulation study

The estimation model was tested in terms of ability to a) detect the absence of year effects, b) correctly estimate year effects given various sample sizes, and c) correctly estimate year effects given different levels of process error. This was accomplished using simulated datasets, where the true growth model and year effects were known.

Simulations were used to examine the sensitivity of the ability to estimate year effects to the amount and the quality of data, and hence to determine how much data are needed to gain an accurate representation of the year effects over 150 years. The number of years was chosen such that it was a longer time period than the longevity of the oldest fish, but short enough that the least oldest fish could theoretically span that time. Three life histories were simulated, based on species that were short-lived and fast-growing (e.g. Pacific sardine *Sardinops sagax*), medium-lived and fast-growing (e.g. petrale sole *Eopsetta jordani*), and long-lived and slow-growing (e.g. splitnose rockfish). Each life history had a unique set of base growth parameters (K_{base} and $w_{\infty,base}$) and maximum age. Each combination of life history, amount of data (number of fish, minimum age of all otoliths as a percentage of the maximum age), and amount of individual and process variance constitutes a scenario. 100 datasets were generated for each scenario, and the model fit to each dataset, resulting in 100 replicates per scenario. Table 3.1 shows the values tested for each factor, and each combination of factors that constitutes a scenario.

Operating model

One hundred datasets were generated for each scenario, and the model fit to these data. Table 3.2 shows the parameters used in the data simulation process. Parameter values were obtained by applying an early version of the estimation model to actual splitnose rockfish otolith data (Table 3.1; Black, pers. comm.), with the exception of β_K , which was set to -0.001 instead of $1.9E-27$, in order for there to be some time-varying component to K . The K_{base} and $w_{\infty,base}$ values for splitnose rockfish were used for the long-lived species, while the values for these parameters for the other life histories were arbitrarily chosen. For each individual fish, its birth year, final age, and the age at which

increments first begin were randomly generated from uniform distributions (Table 3.3), although each individual had at least three growth increments, and increments were bounded to be greater than zero. Year effects ε_t were also randomly generated with an autoregressive lag-1 (AR-1) process, adapted from Thorson et al. (2014):

$$\varepsilon_t = \begin{cases} \rho\varepsilon_{t-1} + \sqrt{1-\rho^2}\omega_t & \text{for } t>1 \\ \omega_t & \text{for } t=1 \end{cases}$$

$$\omega_t \sim \text{Normal}\left(\frac{-1}{2} \times \frac{1-\rho}{\sqrt{1-\rho^2}}, 1\right) \quad (3)$$

where $\rho_{splitnose}$ is the AR-1 coefficient, and ω_t is independent and identically normally distributed variation for year t , with a standard deviation of 1. The year effects used to generate the data were unique to each replicate, and considered the “true” year effects for that replicate. Based on these parameters, Eq. 1 and 2 were used to simulate otolith increment data for each replicate.

Scenarios

Twelve combinations of number of otoliths and minimum age of the otolith (i.e. any otoliths younger than this age were discarded; measured as a proportion of the maximum age), for each of the three life histories, resulting in 36 scenarios (Table 3.2). These factors were selected due to the confounding natures of the individual and year effects, and their values demonstrate a wide range of sample sizes to determine a sample size sufficient to accurately and precisely estimate the year effects. The estimation method was tested in terms of its ability to detect a lack of year effects (i.e. when $\varepsilon_t = 0$ for all t). One data-poor, one data-moderate, and one data-rich scenario were selected (Table 3.4) and 100 datasets were simulated with no year effect. Non-informative starting values

were used for all parameters of the model, except for K_{base} and $w_{\infty,base}$ where the true parameters were used as starting values.

Sensitivity analyses

One data-poor, one data-moderate, and one data-rich scenario (the parameters used to test for detection of non-time-varying growth; Table 3.4) were selected to examine the estimation method's sensitivity to process error. The values tested for the process error parameter σ_{inc} were 0.001, 0.001, 0.01, 0.1, and 0.5.

The data-moderate scenario was used to test the sensitivity to values of σ_K and σ_w . For each parameter, the value ranged from 0.01 to 0.10, in 0.03 increments, and each combination of parameters was tested as a scenario.

The medium-lived species was used to test the sensitivity of the estimation method to the values of β_K and β_w . For β_w , the values tested were 0.001, 0.01, and 0.1, while the values for β_K were set to negative of the same values. Each combination of parameters was tested as a scenario, with varying sample sizes, similar to the data-availability scenarios. In addition, β_K and β_w were set to the values obtained from fitting the published index to weight-at-age data in the stock assessment for splitnose rockfish (Chapter 2; Gertseva et al., 2009), in which β_K was found to be 0.13 and β_w -0.12.

Performance metrics

This model as defined (Eq. 1-3) is susceptible to “label switching” (Redner and Walker, 1984), where two combinations of the three parameters lead to the same likelihood value. Specifically, multiplying the two β parameters and ε_t by -1 results in the same likelihood value. As such, the root mean squared error (RMSE) of the estimated year

effects were calculated twice – once based on the estimated year effects, and once based on a “label switched” estimate of year effects (where ε_t was multiplied by -1) – and the minimum of the two recorded. Based on this result, median absolute error ($AE = \hat{\theta} - \theta$) of the year effects was used to evaluate the performance of the estimation method, where $\hat{\theta}$ represents the estimated value (from the estimation method, either multiplied by -1 or not, depending on RMSE) and θ represents the true value (from the operating model). The correlation between the true time series of year effects and the estimated time series was also investigated using linear regression with the intercept set to 0. The adjusted R^2 value and the median standard deviation of the error (σ) were used to determine the strength of this correlation. The threshold for the correlation between the true time series and the estimated year effects was set as 0.77, as determined by Chapter 2. Median relative errors ($RE = (\hat{\theta} - \theta)/\theta$) of all fixed effect were used to summarize the performance of the estimation method.

RESULTS

Simulation-testing

Scenarios with less informative data (low sample size, minimum age limit, and shorter-lived species) tended to have more runs that failed to converge, where the final gradient of marginal likelihood for each fixed effect was greater than 10^{-6} . This was due in part to there being some years with no data at all (as to be expected in the data-poor situations given a low number of short-lived fish), or the inability to find suitable parameters to fit to the data. Additionally, more replicates failed to converge when the parameters relating to the variances of the random effects (i.e. β_K , $\beta_{w\infty}$, σ_{inc} , σ_K , and σ_w)

were high. In a scenario with actual data, the modeler could tune the estimation method by giving it better starting values. However, given that there were over 8000 replicates in this study, this was not feasible. The ability to obtain unbiased and precise estimates of the year effects also depended on the values for the parameters used to generate the data, particularly those for the same parameters relating to the variance of the random effects. Figure 3.1 shows an example dataset and its corresponding year effects.

The model generally performed well in terms of its ability to recognize and estimate constant, time-invariant growth across the three data-availability scenarios (Figure 3.2). Specifically, median absolute error of year effects were estimated at near zero in the data-poor and data-moderate scenarios, while β_K and β_{w_∞} were estimated very close to zero in the data-moderate and data-rich scenarios. Given that the true values of the year effects and both β_K and β_{w_∞} were zero in the operating model, the absolute errors thus also show that the estimated values were estimated near zero. Overall, the variances of individual effects were imprecisely estimated, regardless of data availability. Accuracy and precision of the fixed effects increased, and bias decreased, with increased data availability.

The number of otoliths sampled had the largest impact on the estimation method's ability to precisely estimate year effects without bias, with the greatest impact on the short-lived species (Figure 3.3). As expected, larger sample sizes led to more accurate and precise estimates of year and fixed effects, and this result holds true for all life histories. Fewer samples (number of otoliths = 20) were required to obtain unbiased year effect estimates for the long-lived species. The estimation method could obtain unbiased and precise estimates of the year effects across all life histories for the largest sample size tested (number of otoliths = 100; Figure 3.3). For the long-lived species, the first few and last few years of the time series were the least precisely-estimated, which was expected

given that there would be more data on the years in the middle of the time series than on the ends. The rate of convergence also increased with longer-lived life history strategies, with a convergence rate of 62-78% in the short-lived species, 69-86% in the medium-lived species, and 85-100% in the long-lived species.

The relationship between estimation performance and the minimum age limit of the otoliths was the most obvious in data-poor scenarios (i.e. when sample sizes were low for the short- and medium-lived species; Figure 3.4). The precision of the year effect estimates increased, and bias decreased when only otoliths from older individuals were available. Base growth parameters (K_{base} and $w_{\infty,base}$) were accurately and precisely estimated across scenarios.

Sensitivity to error

The ability to accurately estimate the year effects was highly sensitive to the value of σ_{inc} (i.e. the extent of process error) in all three data-availability scenarios, with higher values for σ_{inc} reducing precision and increasing the bias of year effect and fixed effect estimates (Figure 3.5). As σ_{inc} (process error) increased, the estimated year effects were increasingly unable to explain the true year effects, and median R^2 value for the year effects decreased (Figure 3.5(c)). Process error is usually described as the natural variation within a population, driven by abiotic or biotic processes not modelled within the population model (Ahrestani et al., 2013). As process error increases, the model increasingly becomes less able to explain the underlying processes driving the population dynamics, and as such the estimation performance of the year effects decreases, particularly after σ_{inc} was greater than 0.01. This was also what likely led to the decrease in the number of replicates that converged as σ_{inc} increased.

Increasing individual effects (σ_K and σ_w) reduced the precision and increased bias of year effect and fixed effect estimates (Figure 3.6). The rate of convergence increased with increasing values of σ_K , but increasing values of σ_w had no discernable effect on the convergence rate. The value for β_w appears to have a larger impact on the accuracy of the year effect estimates than β_K (Figure 3.7). Increasing the values of β_w also increased the proportion of replicates that converged. At high values of β_w , given a sample size of 50 or more, increasing the value of β_K does little to improve the accuracy and precision of the year effect estimates. At low β_w , increased β_K values and increasing sample size reduced the bias of year effect estimates, but the sample size had to be greater than 100 (Figure 3.7). When β_K and β_w were set to stock assessment values (Chapter 2), convergence was low, although the year effect estimates from the converged replicates showed sensitivity to sample size (Figure 3.8). The lack of convergence, as mentioned previously, could have been due to the model's sensitivity to uninformative starting values, and could have required more tuning by hand.

Comparison to the index from Black (2009)

The full model that included year and individual effects on K and w_∞ performed best when fitted to observed data for splitnose rockfish, in that it had the lowest AICc value (Table 3.5). The fits to data are shown in Figure 3.9, and visually it seems that the full model was able to predict observed increment growth for individual otoliths least error. The next best model had only individual effects on K (i.e. $\beta_K = 0$), with a $\Delta AICc$ value of 6 (Table 3.5). As β_K was estimated to be very close to 0 in the full model, this low $\Delta AICc$ value for the model with no β_K was indicative of the model's convergence at a global maximum likelihood. This low β_K value could have been due to the fact that early years of

growth (data which would be most informative to K) were removed from the dataset. As a result, model configurations that estimated K as a constant were also tested (i.e., excluding both individual and annual variation in growth K), but not found to fit the data any better ($\Delta\text{AICc} = 672$; Table 3.5). Comparatively, the model with constant growth (i.e., without individual or annual variation in both K and w_∞), despite having the least parameters, performed poorly relative to the other models ($\Delta\text{AICc} = 2262$; Table 3.5).

An AR-1 model was fit to the estimated year effects for each model configuration that estimated year effects, as was done in Black et al. (2005), and the residuals were linearly regressed to the published index (Figure 3.10). The year effects from the model with time-invariant K (i.e., where the environmental only affected w_∞) was more highly correlated with the published index ($R^2 = 0.64$) compared with the full model ($R^2 = 0.57$), although both correlations were highly statistically significant ($p < 0.001$; Table 3.5).

DISCUSSION

The proposed approach was able to correctly detect the presence of, and accurately and precisely estimate, year effects given otolith growth increment data. Across most scenarios, the model was often unable to unbiasedly and precisely estimate the variance of random effects, which was to be expected as there is often little information on the residual variability in random effects. The ability of the estimation method to precisely estimate year effects without bias is sensitive to the parameters used to generate the data. By simulation-testing the model, we gain a better understanding of the circumstances and data requirements under which the model performs well to obtain an unbiased and precise index of time-varying growth.

With the estimated year effects from this proposed model, other (such as AR) models can be fit to the index and the residuals used to compare with other indices such as climate indices (Black et al., 2005; Black, 2009). Previous studies have shown that climate can have different effects on the somatic growth than on the otolithic growth of fish, and that otolith growth does not necessarily scale somatic growth linearly (Campana, 1990). For example, somatic growth (fish length) is more dependent on food availability for juvenile King George whiting (*Sillaginodes punctatus*), while changes in otolith growth are more closely related to changes in temperature (Barber and Jenkins, 2001). The latter study, though, was conducted only on juvenile fish for a short period of time (several days). A long-term otolith chronology of mature yellowfin sole *Limanda aspera* was also poorly correlated with individual fish body size, though it was able to capture anomalies in the body mass indices of the entire population (Black et al., 2013). Particularly considering that the growth rate parameter estimated in this model do not match the values obtained from the stock assessment of splitnose rockfish ($K = 0.02$ in this study, $K = 0.228$ in Gertseva et al. (2009)), it would be important to fit the derived otolith index to weight-at-age data in a stock assessment to understand its effects on the population's dynamics. By assuming that a time-varying otolith-growth index approximately scales variations in somatic (body) growth, the residual index could potentially be used to inform growth in stock assessment, and improve model fit to weight-at-age data. Work in Chapter 2 found that the value of β strongly influences the decision to include an index of growth in assessments. When β is high, and growth variation is large, the index has to be up to 77% accurate, which could be achieved with a sample size of 20 otoliths, if the species in question was long-lived. A sample size of 100 otoliths would be ideal, as precise and unbiased year effect estimates would be obtained

regardless of life history characteristics. If the β values from fitting the index to weight-at-age data are below 0.3, the index should be included in the assessment anyway, as it is expected to improve overall estimates of spawning stock biomass and recruitment (Chapter 2).

This method was only applied to one set of actual otolith data, and one particular relationship between growth and the environment, and, as in Thorson et al. (2015), the results would only represent populations where these model assumptions are approximately true. The effects of model structure misspecification (e.g. estimating a von Bertalanffy growth function when in fact fish growth follows a Gompertz curve (Gompertz, 1825)) were not explored in this study. The model's ability to detect sexual dimorphic growth (as is the case in splitnose rockfish; Gertseva et al., 2009)) was also not tested in this study, although this could presumably be done in future studies by dividing the data set into two components (male and female) and conducting the analysis separately for each sex. Furthermore, this model assumes that age is known without error, when ageing error is a common problem in stock assessments (Punt et al., 2008). The magnitude of measurement error would be very difficult to quantify in this model, but cross-validation of the otoliths (as described in Black et al., 2005) as well as repeated measurements of the otolith widths might be able to minimize this source of error. Finally, due to the covariance in individual variation and annual variation, it could be possible that the model is sensitive to transient (annually-varying) variation in individual growth, and future studies could estimate whether this component of growth is sufficiently large to impact estimation performance for marine fishes (e.g., Webber and Thorson, 2016).

Applying this approach to other otolith increment data, such as halibut from Weisberg et al. (2010), would increase our understanding of the drivers behind growth in

fish, particularly due to its sensitivity to the operating model. The correlation between otolithic and somatic growth is species-dependent (Ashworth et al., 2016), with this relationship being even more tenuous in tropical fish (Booth, 2014). Hence, this method might not be appropriate for those species. As was done in Black (2009) and Coulson et al. (2014), indices obtained from fitting this model to different species within a geographic region can be compared to identify meaningful relationships across species and climate variables. Furthermore, there has been increasing evidence showing spatial variation in growth (e.g. Rahikainen and Stephenson, 2004; Thorson, 2015), and the model could potentially be expanded to include a spatial component.

The year effects estimated in this study for splitnose rockfish were also correlated with regional climate indices such as the Multivariate El Niño Southern Oscillation Index (MEI) and Pacific Decadal Oscillation (PDO), as described in Black (2009). In light of projected increasing ocean temperatures (Kirtman et al., 2013), it can be expected that climate will continue to impact growth and other aspects of marine fish populations in the future. It is vital that we increase our understanding of time-varying impacts on population dynamics, to reduce model structure uncertainty and to increase forecasting ability. While the proposed model assumes a constant relationship between climate and fish growth, this might not always be the case (Webber and Thorson, 2016), climate and disturbance histories reconstructed using tree-ring data have generally been accurate (e.g. Baker et al., 2005; Esper et al., 2002; Fritts, 1991), despite having similar assumptions. Furthermore, correlations between otolith widths and tree ring increments have previously been found (Black, 2009; Guyette and Rabeni, 1995), which supports the assumption that the environment will continue affecting fish growth in a similar manner (Morrongiello et al., 2011).

Otoliths contain a wealth of information, and continue to be used an important resource in the management of fisheries (Begg et al., 2005). In this study, we have proposed and simulation-tested a novel method of analyzing otolith data to estimate time-varying growth; using a von Bertalanffy growth curve with random individual and year effects. By applying this method to otolith data, time-varying indices of growth could be obtained and potentially be used in stock assessments. The mechanistic drivers behind time-varying growth still warrant exploration, and the indices estimated from this model can be used as a first step towards investigating the relationship between climate and growth.

TABLES

Table 3.1 Description of the parameters used in the model.

Symbol	Description	Value
<u>Fixed Effects</u>		
K_{base}	von Bertalanffy growth coefficient (yr ⁻¹ ; Eq 1)	Varies per life history
$w_{\infty,base}$	Asymptotic length (mm; Eq 1)	Varies per life history
β_K	Multiplicative link parameter to K	-0.001
$\beta_{w_{\infty}}$	Multiplicative link parameter to w_{∞}	0.008
σ_{inc}	Standard deviation of increment measurements	0.0003
σ_K	Standard deviation of individual effects on K	0.05
σ_w	Standard deviation of individual effects on w_{∞}	0.03
<u>Random Effects</u>		
$\varepsilon_{K,i}$	Individual effects on K	Normal(0, σ_K)
$\varepsilon_{w_{\infty},i}$	Individual effects on w_{∞}	Normal(0, σ_w)
ε_t	Year effects	Normal(0, 1)

Table 3.2 Description of life histories used and their associated parameters.

Life Histories	Maximum Age (years)	K (yr⁻¹)	w_{∞} (mm)
Short-lived, fast-growing	15	0.2	1
Medium-lived, medium-growing	25	0.1	1.5
Long-lived, slow-growing	100	0.02	2.3
Scenarios Tested	Values		
Number of otoliths	20, 50, 100		
Minimum age (proportion of maximum age)	0.1, 0.3, 0.5, 0.7		

Table 3.3 Description of uniform distributions used to generate data.

Randomly-generated data	Minimum Value	Maximum Value
Initial age of otolith (age at which otolith increments start being measured and recorded)	1 year	0.1 of maximum age
Final age of otolith	Minimum age of otolith (Table 3.2)	Maximum age of otolith (Table 3.1)
Number of increments	3	Final age - initial age
First year from which increments begin	1	Total years (150) - number of increments

Table 3.4 Values used in sensitivity analyses

Scenarios	Life History	Number of fish	Minimum age of otolith (proportion of maximum age)
Data-poor	Short-lived, fast-growing	20	0.1
Data-moderate	Medium-lived, medium-growing	20	0.7
Data-rich	Long-lived, slow-growing	100	0.7

Table 3.5 Fixed effect estimates and AICc values for each model configuration fit to the actual data splitnose rockfish. The R^2 and the estimated variance of error values result from fitting the estimated year effects to the index published by Black (2009).

Model	K_{base}	$w_{\infty, base}$ (mm)	β_K	$\beta_{w_{\infty}}$	σ_{inc}	σ_K	σ_w	R^2 (year effects)	Error (year effects)	AICc	$\Delta AICc$
All effects - individual and year	0.02	2.35	0.46	0.06	0.00	0.50	0.34	0.5725 (p<0.001)	0.6492	-20674	0
No individual or year effects	0.01	2.87	NA	NA	0.01	NA	NA	NA	NA	-18412	2262
Just individual effects	0.01	2.85	NA	NA	4.16E-03	0.43	0.29	NA	NA	-19931	743
Just year effects	0.01	3.05	0.46	-0.24	0.01	NA	NA	0.5453 (p<0.001)	0.6696	-18664	2011
No year effects on K	0.02	2.34	NA	-0.09	3.31E-03	0.50	0.34	0.5454 (p<0.001)	0.6695	-20669	6
Constant K	0.02	2.56	NA	-0.06	4.11E-03	NA	0.16	0.6427 (p<0.001)	0.5935	-20002	672

FIGURES

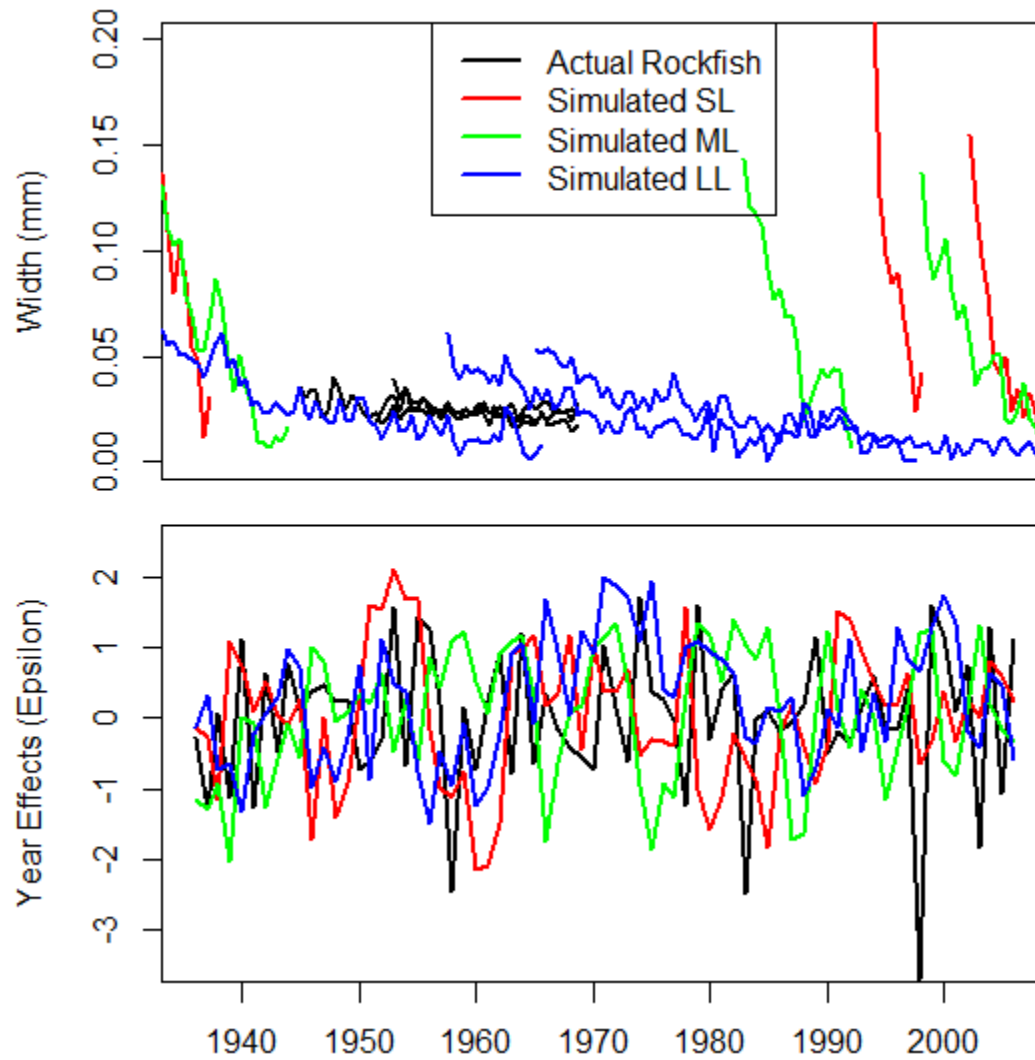


Figure 3.1 Example increment growth curves for each life history, and the corresponding year effects.

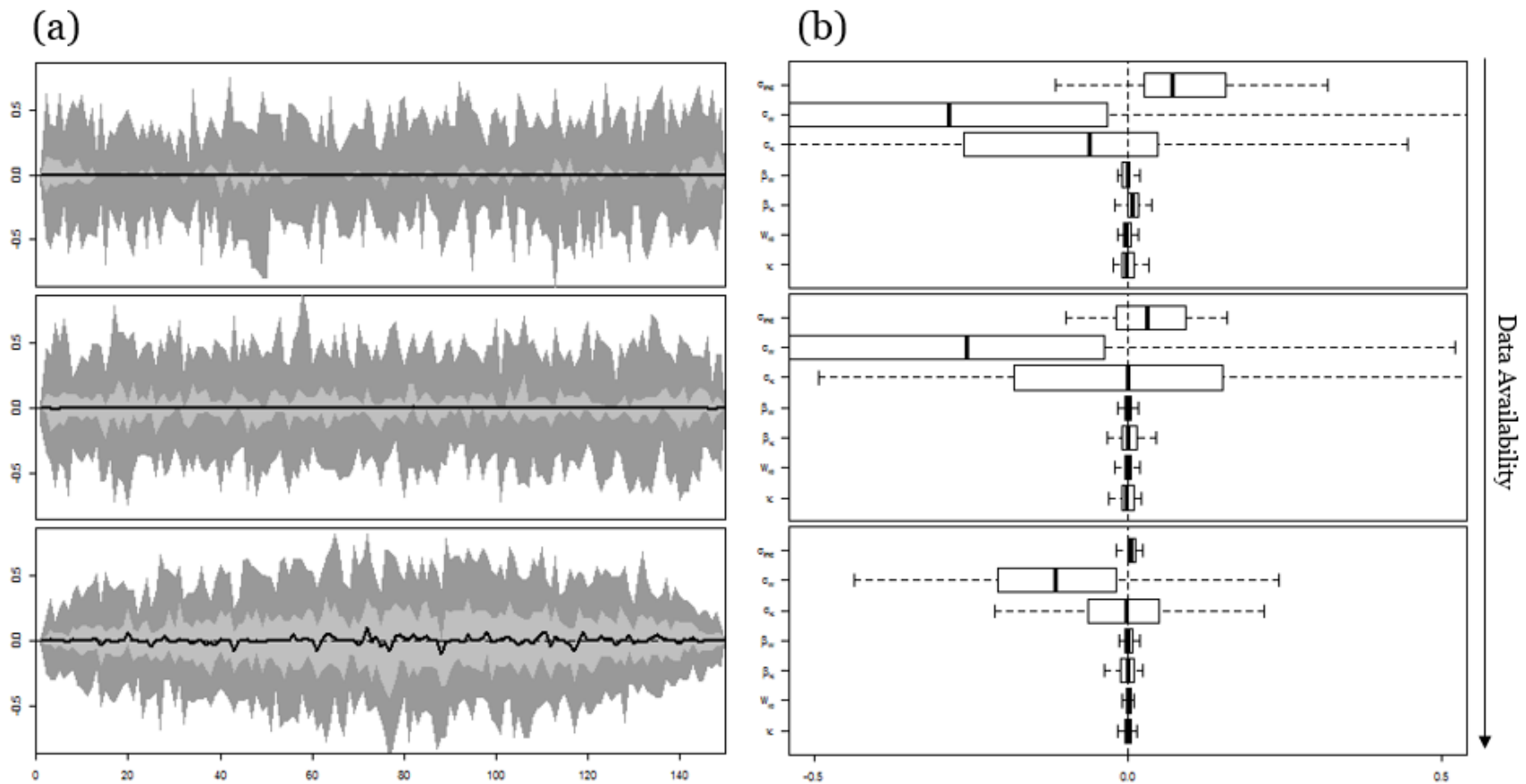


Figure 3.2 Summary of results from the scenarios where there was no year effect. Each row represents a life history strategy: top to bottom short-lived to long-lived. Panel (a) shows the absolute error of estimated year effects. The solid black line represents the median absolute error, while the light gray and dark gray areas show the 50% and 95% simulation intervals respectively. The dashed black line shows the zero line. Panel (b) shows a boxplot of the relative errors of estimated fixed effects. As the true values of both β parameters are zero, the absolute error for these parameters

are shown. The solid black line represents the median relative error, while boxes show the first and third quantiles. The whiskers show the 95% simulation intervals. The dashed black line shows the zero line.

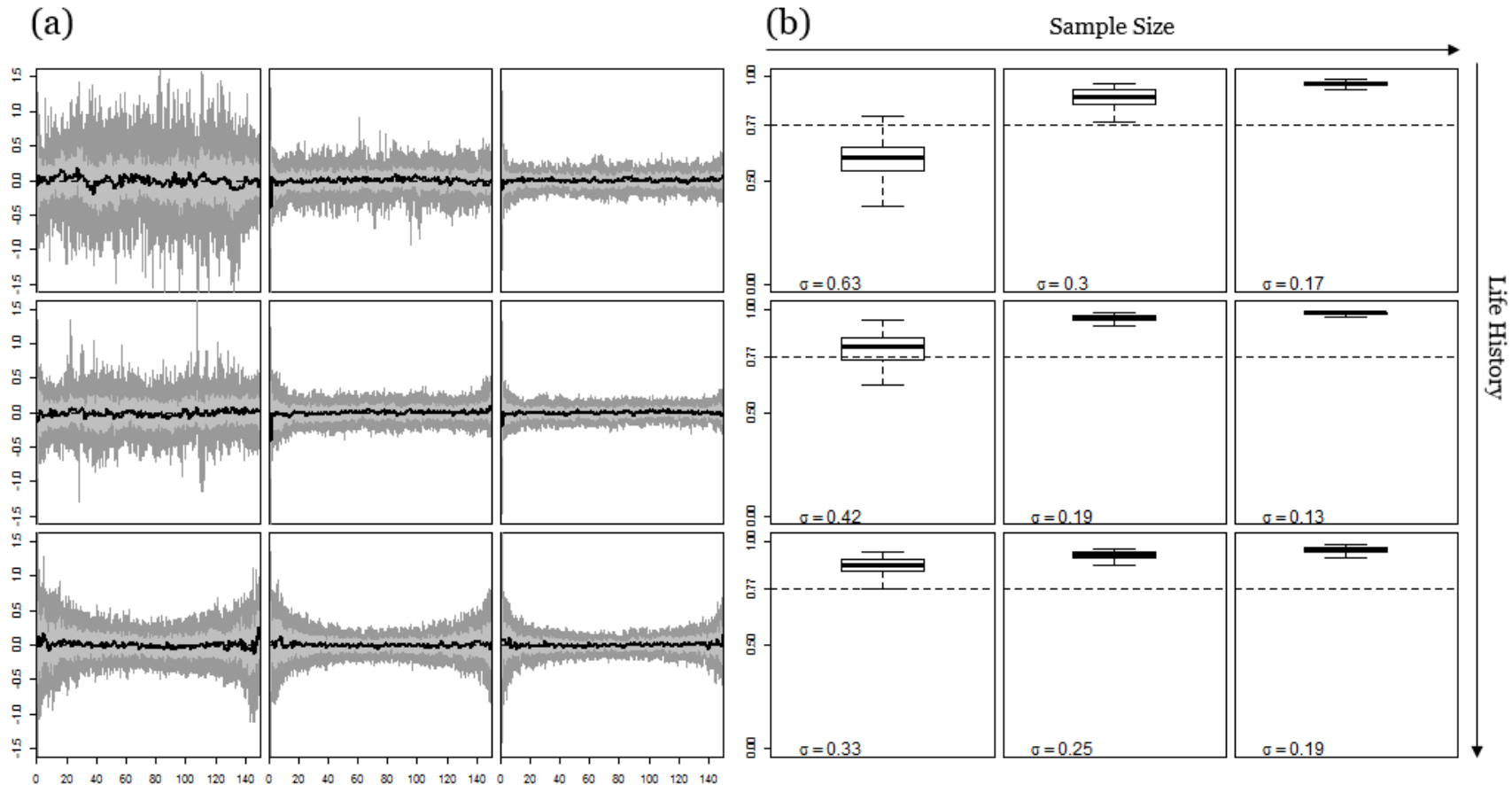


Figure 3.3 Summary of results from the sensitivity analysis of year effect estimates to sample size, for a minimum age limit of 0.3 of the maximum age. Each column in a panel represents a sample size, increasing from left to right. Each row represents a life history strategy: top to bottom short-lived to long-lived. Panel (a) shows the absolute error of estimated year effects. The solid black line represents the median absolute error, while the light gray and dark gray areas show the 50% and 95% simulation intervals respectively. The dashed black line shows the zero line. Panel (b) shows boxplots of the R^2 value from fitting a linear regression model to test the relationship between the true and the estimated year effects. The

solid black line represents the median relative error, while the boxes show the first and third quantiles. The whiskers show the 95% simulation intervals. The dashed black line shows the 0.77 value (obtained from Chapter 2).

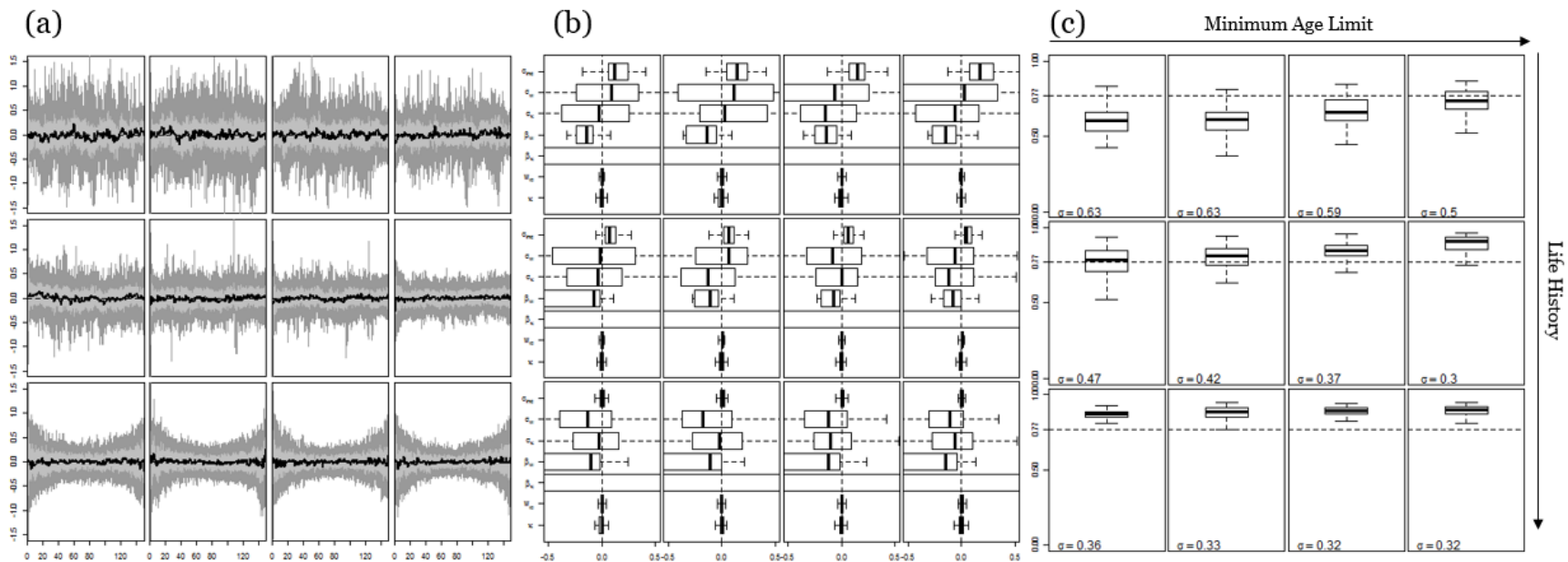


Figure 3.4 Summary of results from the sensitivity analysis to minimum age limit at a sample size of 20, the lowest sample size tested. Each row within a panel represents a life history strategy: top to bottom short-lived to long-lived. Each column represents a value of minimum age limit. Panel (a) shows the absolute error of estimated year effects. The solid black line represents the median absolute error, while the light gray and dark gray areas show the 50% and 95% simulation intervals respectively. The dashed black line shows the zero line. Panel (b) shows boxplots of the relative errors of estimated fixed effects. The solid black line represents the median relative error, while the boxes show the first and third quartiles. The whiskers show the 95% simulation intervals. The dashed black line shows the zero line. Panel (c) shows boxplots of the R² value from fitting a linear regression model to test the relationship between the true and the estimated year effects. The dashed black line shows the 0.77 value (obtained from Chapter 2).

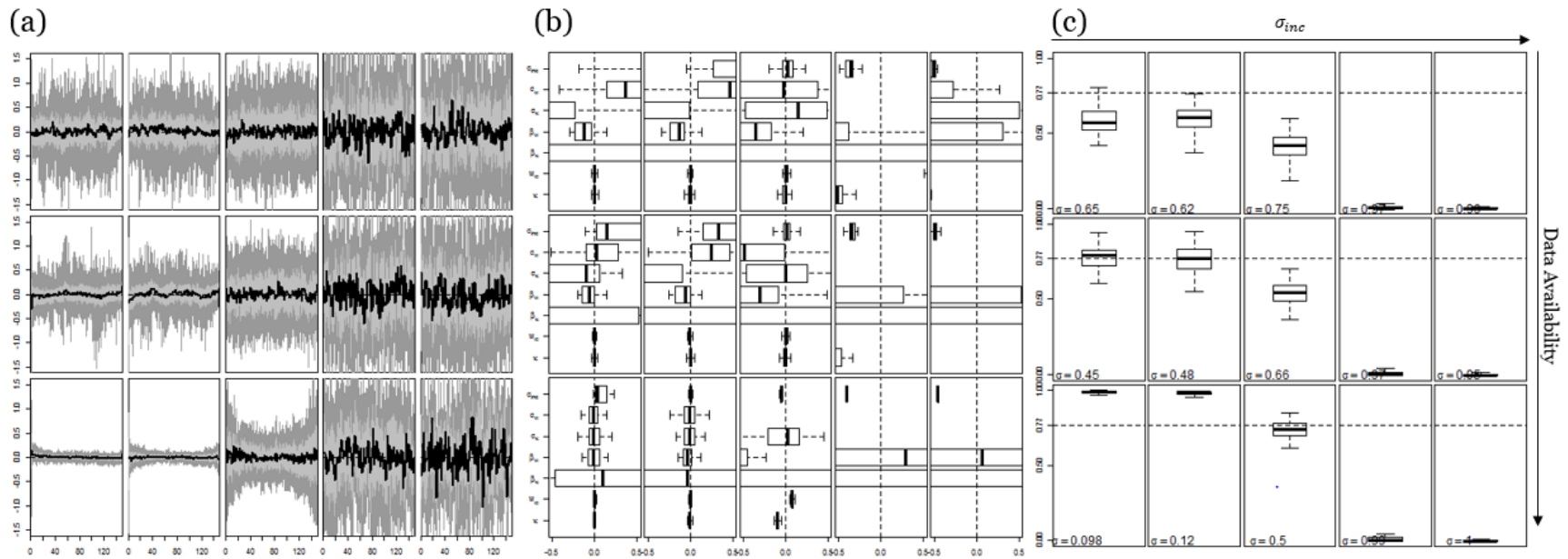


Figure 3.5 Summary of results from the sensitivity analysis to the value of σ_{inc} . Each row represents a data-availability scenario: top to bottom data-poor to data-rich. Each column represents a value of σ_{inc} , increasing from left to right. Panel (a) shows the absolute error of estimated year effects. The solid black line represents the median absolute error, while the light gray and dark gray areas show the 50% and 95% simulation intervals respectively. The dashed black line shows the zero line. Panel (b) shows boxplots of the relative errors of estimated fixed effects. The solid black line represents the median relative error, while the boxes show the first and third quartiles. The whiskers show the 95% simulation intervals. The dashed black line shows the zero line. Panel (c) shows boxplots of the R^2 value from fitting a linear regression model to test the relationship between the true and the estimated year effects. The dashed black line shows the 0.77 value (obtained from Chapter 2).

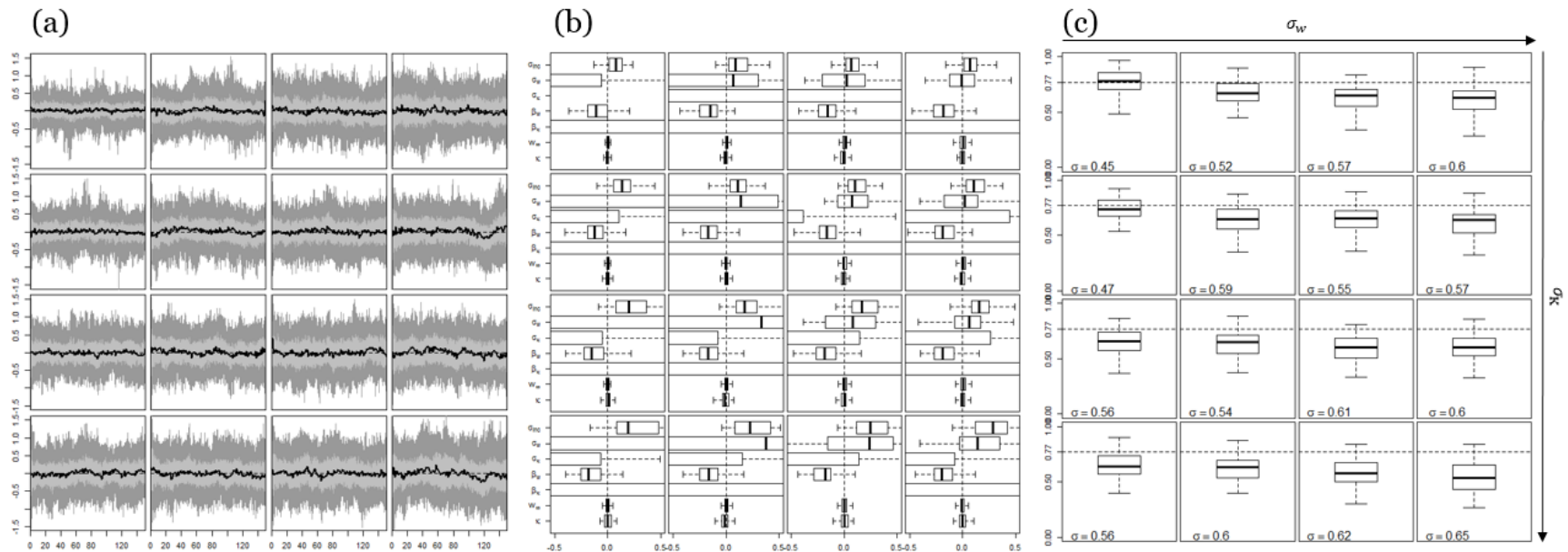


Figure 3.6 Summary of results from the sensitivity analysis to the values for σ_w and σ_K . Each row represents a value for σ_K , increasing from top to bottom. Each column represents a value of σ_w , increasing from left to right. Panel (a) shows the absolute error of estimated year effects. The solid black line represents the median absolute error, while the light gray and dark gray areas show the 50% and 95% simulation intervals respectively. The dashed black line shows the zero line. Panel (b) shows boxplots of the relative errors of estimated fixed effects. The solid black line represents the median relative error, while boxes show the first and third quantiles. The whiskers show the 95% simulation intervals. The dashed black line shows the zero line. Panel (c) shows boxplots of the R^2 value from fitting a linear regression model to test the relationship between the true and the estimated year effects. The dashed black line shows the 0.77 value (obtained from Chapter 2).

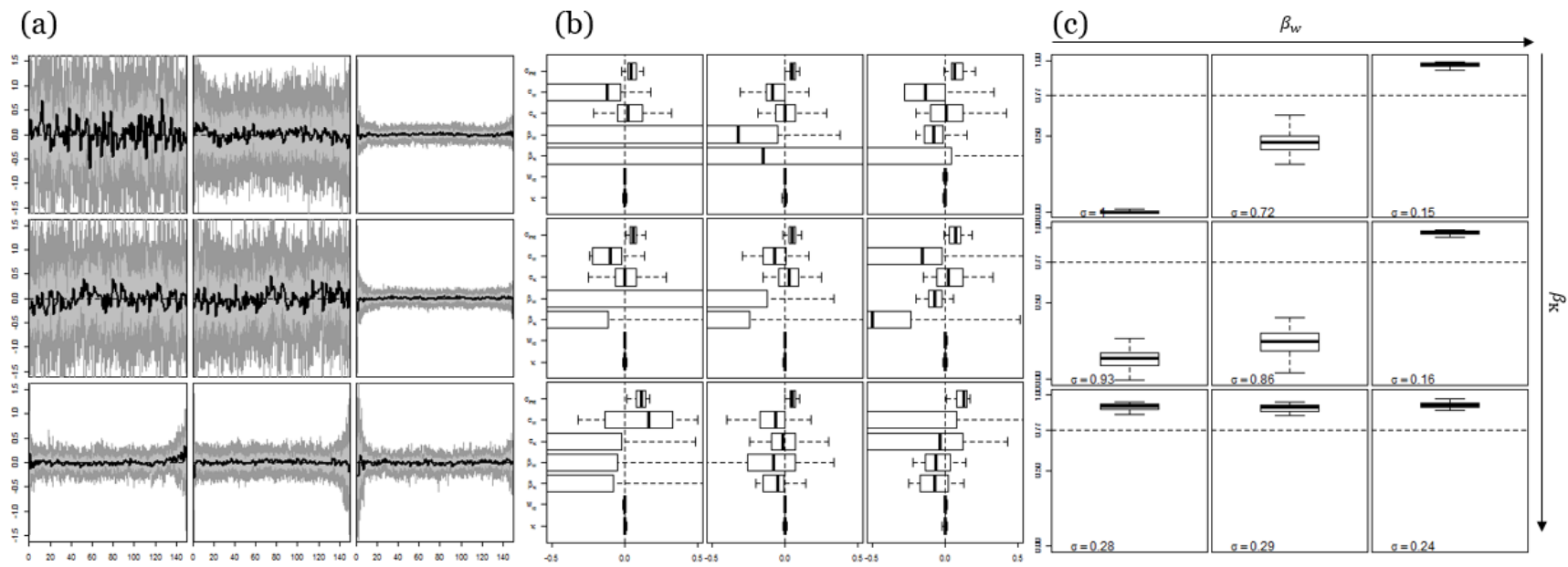


Figure 3.7 Summary of results from the sensitivity analysis to the values for β_w and β_K , at a sample size of 100. Each row within a panel represents a value for β_K , increasing from top to bottom. Each column represents a value of β_w , increasing from left to right. Panel (a) shows the absolute error of estimated year effects. The solid black line represents the median absolute error, while the light gray and dark gray areas show the 50% and 95% simulation intervals respectively. The dashed black line shows the zero line. Panel (b) shows boxplots of the relative errors of estimated fixed effects. The solid black line represents the median relative error, while boxes show the first and third quantiles. The whiskers show the 95% simulation intervals. The dashed black line shows the zero line. Panel (c) shows boxplots of the R² value from fitting a linear regression model to test the relationship between the true and the estimated year effects. The dashed black line shows the 0.77 value (obtained from Chapter 2).

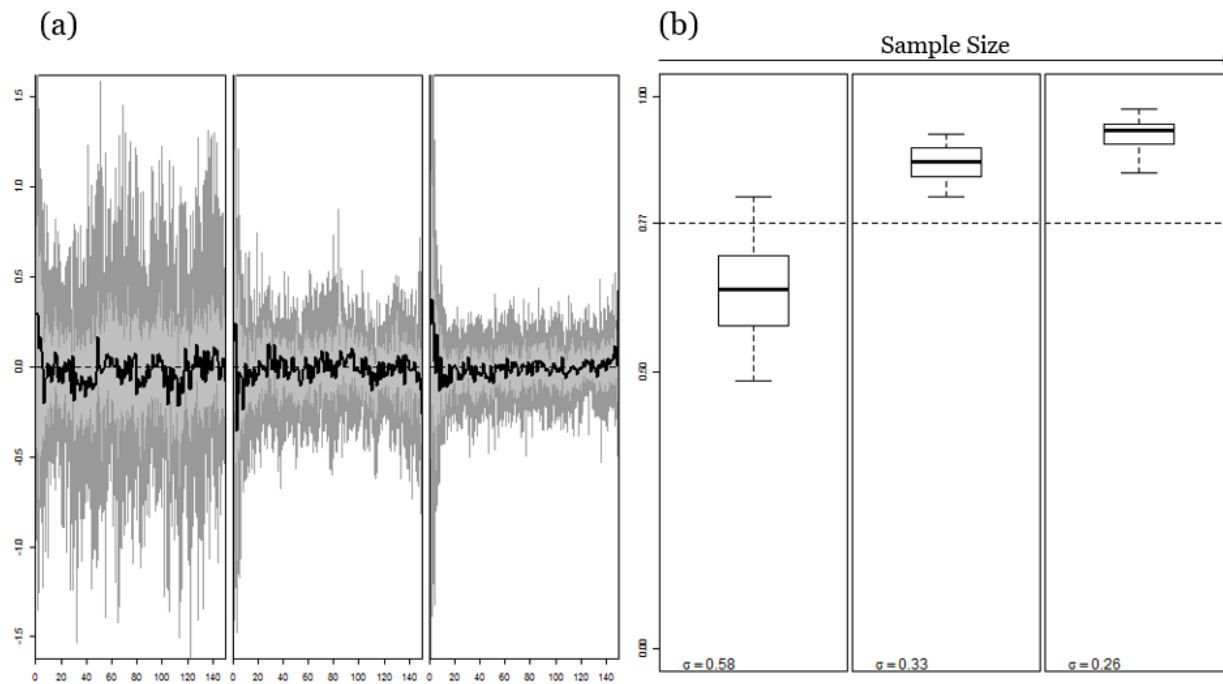


Figure 3.8 Summary of results of setting for β_w and β_K to the stock assessment values, where the signs are inverted. Each column represents a different sample size. Panel (a) shows the absolute error of estimated year effects. The solid black line represents the median absolute error, while the light gray and dark gray areas show the 50% and 95% simulation intervals respectively. The dashed black line shows the zero line. Panel (b) shows boxplots of the R^2 value from fitting a linear regression model to test the relationship between the true and the estimated year effects. The dashed black line shows the 0.77 value (obtained from Chapter 2).

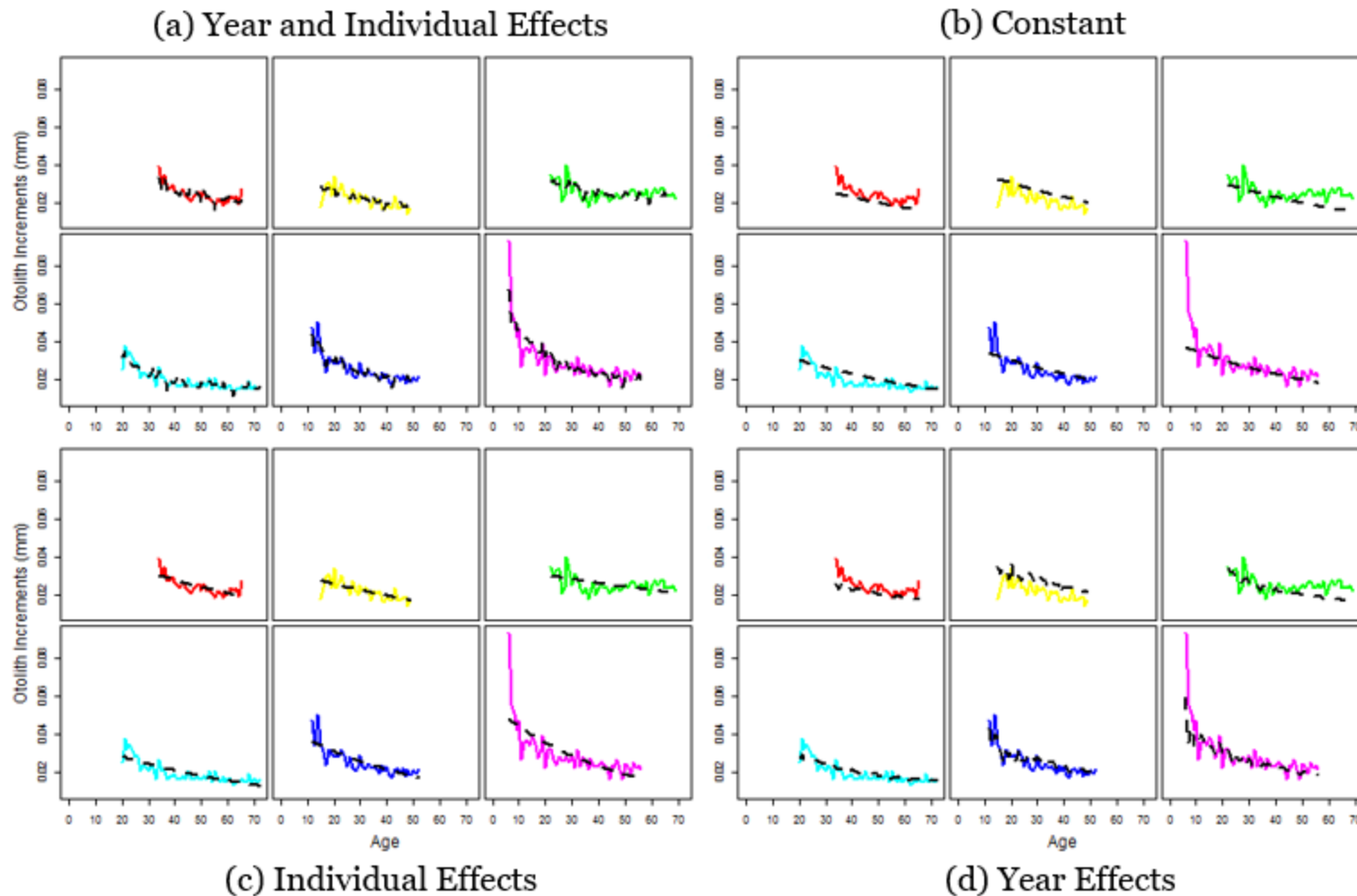


Figure 3.9 Model fits to actual otolith increment data for 6 individual splitnose rockfish, selected out of the total sample size of 66. The solid lines represent the data, with each color representing an individual, while the dashed black line represents model predictions.

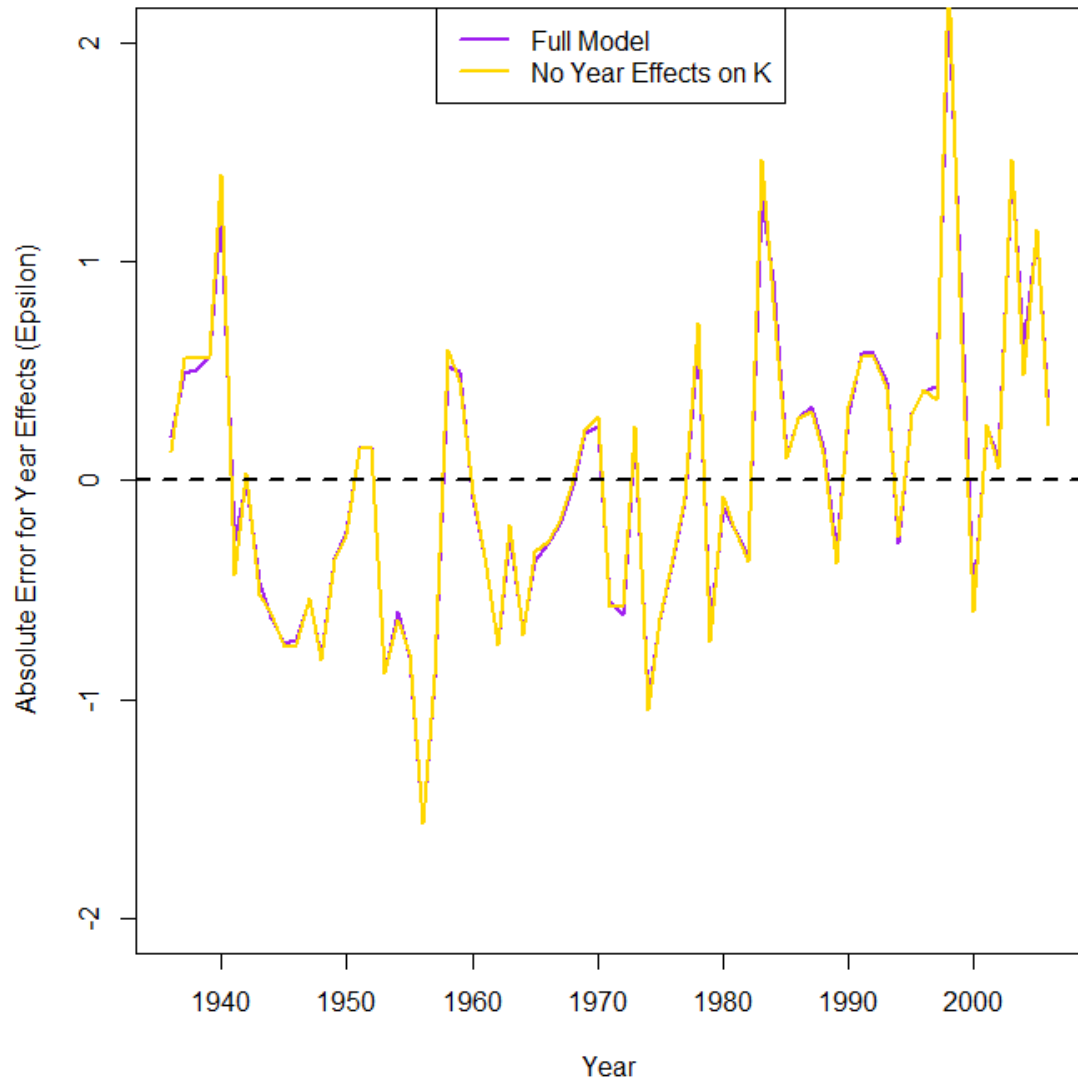


Figure 3.10 Difference (absolute error) between estimated year effects from fitting the proposed model to the actual otolith data, compared with the published index from Black (2009). The dashed black line represents the zero line.

BIBLIOGRAPHY

- Ahrestani, Farshid S., Mark Hebblewhite, and Eric Post. “The Importance of Observation versus Process Error in Analyses of Global Ungulate Populations.” *Scientific Reports* 3 (November 8, 2013): 3125. doi:10.1038/srep03125.
- Ait Youcef, Wahiba, Yvan Lambert, and Céline Audet. “Variations in Length and Growth of Greenland Halibut Juveniles in Relation to Environmental Conditions.” *Fisheries Research* 167 (July 2015): 38–47. doi:10.1016/j.fishres.2015.01.007.
- A’mar, Z. Teresa, André E. Punt, and Martin W. Dorn. “The Evaluation of Two Management Strategies for the Gulf of Alaska Walleye Pollock Fishery under Climate Change.” *ICES Journal of Marine Science: Journal Du Conseil* 66, no. 7 (August 1, 2009): 1614–32. doi:10.1093/icesjms/fsp044.
- Ashworth, Eloïse C., Norman G. Hall, S. Alex Hesp, Peter G. Coulson, and Ian C. Potter. “Age and Growth Rate Variation Influence the Functional Relationship between Somatic and Otolith Size.” *Canadian Journal of Fisheries and Aquatic Sciences* 74, no. 5 (September 16, 2016): 680–92. doi:10.1139/cjfas-2015-0471.
- Baker, Patrick J., Sarayudh Bunyavejchewin, Chadwick D. Oliver, and Peter S. Ashton. “Disturbance History and Historical Stand Dynamics of a Seasonal Tropical Forest in Western Thailand.” *Ecological Monographs* 75, no. 3 (February 1, 2005): 317–43. doi:10.1890/04-0488.
- Ballagh, Aaron C., David Welch, Ashley J. Williams, Amos Mapleston, Andrew Tobin, and Nicholas Marton. “Integrating Methods for Determining Length-at-Age to Improve Growth Estimates for Two Large Scombrids.” *Fishery Bulletin* 109, no. 1 (2011): 90–100.
- Barber, M. C., and G. P. Jenkins. “Differential Effects of Food and Temperature Lead to Decoupling of Short-Term Otolith and Somatic Growth Rates in Juvenile King George Whiting.” *Journal of Fish Biology* 58, no. 5 (May 1, 2001): 1320–30. doi:10.1111/j.1095-8649.2001.tb02289.x.

- Basson, M. "The Importance of Environmental Factors in the Design of Management Procedures." *ICES Journal of Marine Science: Journal Du Conseil* 56, no. 6 (December 1, 1999): 933–42. doi:10.1006/jmsc.1999.0541.
- Begg, Gavin A., Steven E. Campana, Anthony J. Fowler, and Iain M. Suthers. "Otolith Research and Application: Current Directions in Innovation and Implementation." *Marine and Freshwater Research* 56, no. 5 (August 9, 2005): 477–83. doi:10.1071/MF05111.
- Biro, Peter A., Christa Beckmann, and Judy A. Stamps. "Small within-Day Increases in Temperature Affects Boldness and Alters Personality in Coral Reef Fish." *Proceedings of the Royal Society of London B: Biological Sciences* 277, no. 1678 (January 7, 2010): 71–77. doi:10.1098/rspb.2009.1346.
- Black, Bryan A. "Climate-Driven Synchrony across Tree, Bivalve, and Rockfish Growth-Increment Chronologies of the Northeast Pacific." *Marine Ecology Progress Series* 378 (March 12, 2009): 37–46. doi:10.3354/meps07854.
- Black, Bryan A., George W. Boehlert, and Mary M. Yoklavich. "Establishing Climate-growth Relationships for Yelloweye Rockfish (*Sebastes Ruberrimus*) in the Northeast Pacific Using a Dendrochronological Approach." *Fisheries Oceanography* 17, no. 5 (September 1, 2008): 368–79. doi:10.1111/j.1365-2419.2008.00484.x.
- Black, Bryan A, George W Boehlert, and Mary M Yoklavich. "Using Tree-Ring Crossdating Techniques to Validate Annual Growth Increments in Long-Lived Fishes." *Canadian Journal of Fisheries and Aquatic Sciences* 62, no. 10 (October 1, 2005): 2277–84. doi:10.1139/f05-142.
- Black, Bryan A., Mary E. Matta, Thomas E. Helser, and Thomas K. Wilderbuer. "Otolith Biochronologies as Multidecadal Indicators of Body Size Anomalies in Yellowfin Sole (*Limanda Aspera*)." *Fisheries Oceanography* 22, no. 6 (November 1, 2013): 523–32. doi:10.1111/fog.12036.
- Booth, D. J. "Do Otolith Increments Allow Correct Inferences about Age and Growth of Coral Reef Fishes?" *Coral Reefs* 33, no. 1 (March 1, 2014): 255–58. doi:10.1007/s00338-013-1105-2.

- Brander, Keith. "Impacts of Climate Change on Fisheries." *Journal of Marine Systems*, Impact of climate variability on marine ecosystems: A comparative approach, 79, no. 3–4 (February 10, 2010): 389–402. doi:10.1016/j.jmarsys.2008.12.015.
- Brander, Keith M. "The Role of Growth Changes in the Decline and Recovery of North Atlantic Cod Stocks since 1970." *ICES Journal of Marine Science* 64, no. 2 (March 1, 2007): 211–17. doi:10.1093/icesjms/fsl021.
- Brett, J. R. "10 - Environmental Factors and Growth." In *Fish Physiology*, edited by D. J. Randall and J. R. Brett W.S. Hoar, 8:599–675. Bioenergetics and Growth. Academic Press, 1979. doi:10.1016/S1546-5098(08)60033-3.
- Brunel, Thomas, and Mark Dickey-Collas. "Effects of Temperature and Population Density on von Bertalanffy Growth Parameters in Atlantic Herring: A Macro-Ecological Analysis." *Marine Ecology Progress Series* 405 (2010): 15–28. doi:10.3354/meps08491.
- Campana, Steven E. "Chemistry and Composition of Fish Otoliths: Pathways, Mechanisms and Applications." *Marine Ecology Progress Series* 188 (November 3, 1999): 263–97. doi:10.3354/meps188263.
- . "How Reliable Are Growth Back-Calculations Based on Otoliths?" *Canadian Journal of Fisheries and Aquatic Sciences* 47, no. 11 (November 1, 1990): 2219–27. doi:10.1139/f90-246.
- Coulson, P. G., B. A. Black, I. C. Potter, and N. G. Hall. "Sclerochronological Studies Reveal That Patterns of Otolith Growth of Adults of Two Co-Occurring Species of Platycephalidae Are Synchronised by Water Temperature Variations." *Marine Biology* 161, no. 2 (February 1, 2014): 383–93. doi:10.1007/s00227-013-2343-0.
- Dale, Katherine E., Elizabeth A. Daly, and Richard D. Brodeur. "Interannual Variability in the Feeding and Condition of Subyearling Chinook Salmon off Oregon and Washington in Relation to Fluctuating Ocean Conditions." *Fisheries Oceanography*, September 1, 2016, n/a-n/a. doi:10.1111/fog.12180.
- Escati-Peñaloza, Gabriela, Ana M. Parma, and J. M. (Lobo) Orensanz. "Analysis of Longitudinal Growth Increment Data Using Mixed-Effects Models: Individual and Spatial Variability in a Clam." *Fisheries Research* 105, no. 2 (July 2010): 91–101. doi:10.1016/j.fishres.2010.03.007.

- Esper, Jan, Edward R. Cook, and Fritz H. Schweingruber. "Low-Frequency Signals in Long Tree-Ring Chronologies for Reconstructing Past Temperature Variability." *Science* 295, no. 5563 (March 22, 2002): 2250–53. doi:10.1126/science.1066208.
- Essington, Timothy E., James F. Kitchell, and Carl J. Walters. "The von Bertalanffy Growth Function, Bioenergetics, and the Consumption Rates of Fish." *Canadian Journal of Fisheries and Aquatic Sciences* 58, no. 11 (November 2001): 2129–38.
- Fournier, David, and Chris P. Archibald. "A General Theory for Analyzing Catch at Age Data." *Canadian Journal of Fisheries and Aquatic Sciences* 39, no. 8 (August 1, 1982): 1195–1207. doi:10.1139/f82-157.
- Francis, R. I. C. Chris. "Growth in Age-Structured Stock Assessment Models." *Fisheries Research*, Growth: theory, estimation, and application in fishery stock assessment models, 180 (August 2016): 77–86. doi:10.1016/j.fishres.2015.02.018.
- Fritts, H. C. (Arizona Univ. "Reconstructing Large-Scale Climatic Patterns from Tree-Ring Data," January 1, 1991. <https://www.osti.gov/scitech/biblio/5321264>.
- Gertseva, Vladlena V., Jason M. Cope, and Donald E. Pearson. "Status of the U.S. Splitnose Rockfish (*Sebastes Diploproa*) Resource in 2009." Status of the Pacific Coast Groundfish Fishery through 2009 and Recommended Acceptable Biological Catches for 2011/2012: Stock Assessment and Fishery Evaluation, 2009. Portland, OR: Pacific Fishery Management Council, October 2009. http://www.pcouncil.org/wp-content/uploads/Splitnose_Rf_2009_SAFE_version.pdf.
- Gertseva, Vladlena V., Jason Marc Cope, and Donald Edgar Pearson. "Status of the US Splitnose Rockfish (*Sebastes Diploproa*) Resource in 2009." Status of the Pacific Coast Groundfish Fishery through 2009 and Recommended Acceptable Biological Catches for 2011/2012: Stock Assessment and Fishery Evaluation, 2009. Portland, OR: Northwest Fisheries Science Center, NOAA Fisheries, October 2009. http://dev.pcouncil.org/wp-content/uploads/Splitnose_Rf_2009_SAFE_version.pdf.
- Gertseva, VV, JM Cope, and SE Matson. "Growth Variability in the Splitnose Rockfish *Sebastes Diploproa* of the Northeast Pacific Ocean: Pattern Revisited." *Marine*

- Ecology Progress Series* 413 (August 26, 2010): 125–36.
doi:10.3354/meps08719.
- Gompertz, Benjamin. “On the Nature of the Function Expressive of the Law of Human Mortality, and on a New Mode of Determining the Value of Life Contingencies.” *Philosophical Transactions of the Royal Society of London* 115 (1825): 513–83.
- Grimm, Volker, Eloy Revilla, Uta Berger, Florian Jeltsch, Wolf M. Mooij, Steven F. Railsback, Hans-Hermann Thulke, Jacob Weiner, Thorsten Wiegand, and Donald L. DeAngelis. “Pattern-Oriented Modeling of Agent-Based Complex Systems: Lessons from Ecology.” *Science* 310, no. 5750 (November 11, 2005): 987–91. doi:10.1126/science.1116681.
- Guyette, Richard P., and Charles F. Rabeni. “Climate Response among Growth Increments of Fish and Trees.” *Oecologia* 104, no. 3 (1995): 272–79.
- Haltuch, Melissa A., and André E. Punt. “The Promises and Pitfalls of Including Decadal-Scale Climate Forcing of Recruitment in Groundfish Stock Assessment.” *Canadian Journal of Fisheries and Aquatic Sciences* 68, no. 5 (May 1, 2011): 912–26. doi:10.1139/f2011-030.
- Harley, Christopher D. G., A. Randall Hughes, Kristin M. Hultgren, Benjamin G. Miner, Cascade J. B. Sorte, Carol S. Thornber, Laura F. Rodriguez, Lars Tomanek, and Susan L. Williams. “The Impacts of Climate Change in Coastal Marine Systems.” *Ecology Letters* 9, no. 2 (February 1, 2006): 228–41. doi:10.1111/j.1461-0248.2005.00871.x.
- Helser, Thomas E, and Jon KT Brodziak. “Impacts of Density-Dependent Growth and Maturation on Assessment Advice to Rebuild Depleted U.S. Silver Hake (*Merluccius Bilinearis*) Stocks.” *Canadian Journal of Fisheries and Aquatic Sciences* 55, no. 4 (April 1, 1998): 882–92. doi:10.1139/f97-290.
- Hollowed, Anne Babcock, Nicholas A. Bond, Thomas K. Wilderbuer, William T. Stockhausen, Z. Teresa A’mar, Richard J. Beamish, James E. Overland, and Michael J. Schirripa. “A Framework for Modelling Fish and Shellfish Responses to Future Climate Change.” *ICES Journal of Marine Science: Journal Du Conseil* 66, no. 7 (August 1, 2009): 1584–94. doi:10.1093/icesjms/fsp057.
- Holt, Carrie A., and André E. Punt. “Incorporating Climate Information into Rebuilding Plans for Overfished Groundfish Species of the U.S. West Coast.” *Fisheries*

- Research, Ecosystem Approach to Fisheries: Improvements on Traditional Management for Declining and Depleted Stocks* Annual Meeting of the North Pacific Marine Science Organization, 100, no. 1 (September 2009): 57–67. doi:10.1016/j.fishres.2009.03.002.
- Hulson, Peter-John F., Terrance J. Quinn, Dana H. Hanselman, and James N. Ianelli. “Spatial Modeling of Bering Sea Walleye Pollock with Integrated Age-Structured Assessment Models in a Changing Environment.” *Canadian Journal of Fisheries and Aquatic Sciences* 70, no. 9 (July 2, 2013): 1402–16. doi:10.1139/cjfas-2013-0020.
- Ianelli, James N., Anne B. Hollowed, Alan C. Haynie, Franz J. Mueter, and Nicholas A. Bond. “Evaluating Management Strategies for Eastern Bering Sea Walleye Pollock (*Theragra Chalcogramma*) in a Changing Environment.” *ICES Journal of Marine Science: Journal Du Conseil* 68, no. 6 (July 1, 2011): 1297–1304. doi:10.1093/icesjms/fsr010.
- Johnson, Kelli F., Cole C. Monnahan, Carey R. McGilliard, Katyana A. Vert-pre, Sean C. Anderson, Curry J. Cunningham, Felipe Hurtado-Ferro, et al. “Time-Varying Natural Mortality in Fisheries Stock Assessment Models: Identifying a Default Approach.” *ICES Journal of Marine Science: Journal Du Conseil*, April 9, 2014, fsu055. doi:10.1093/icesjms/fsu055.
- Kimura, Daniel K. “Extending the von Bertalanffy Growth Model Using Explanatory Variables.” *Canadian Journal of Fisheries and Aquatic Sciences* 65, no. 9 (August 21, 2008): 1879–91. doi:10.1139/F08-091.
- Kirtman, B., S. B. Power, A. J. Adedoyin, G. J. Boer, R. Bojariu, I. Camilloni, F. Doblaser-Reyes, et al. “Chapter 11 - Near-Term Climate Change: Projections and Predictability.” In *Climate Change 2013: The Physical Science Basis. IPCC Working Group I Contribution to AR5*, edited by IPCC. Cambridge: Cambridge University Press, 2013. http://www.climatechange2013.org/images/report/WG1AR5_Chapter11_FINAL.pdf.
- Kristensen, Kasper, Anders Nielsen, Casper W. Berg, Hans J. Skaug, and Bradley M. Bell. “TMB: Automatic Differentiation and Laplace Approximation.” *Journal of Statistical Software* 70, no. 5 (2016): 1–21. doi:10.18637/jss.v070.i05.

- Liang, Kung-Yee, and Scott L. Zeger. "Longitudinal Data Analysis Using Generalized Linear Models." *Biometrika* 73, no. 1 (1986): 13–22. doi:10.2307/2336267.
- López-Abellán, Luis J., María T. G. Santamaría, and José F. González. "Approach to Ageing and Growth Back-Calculation Based on the Otolith of the Southern Boarfish *Pseudopentaceros Richardsoni* (Smith, 1844) from the South-West Indian Ocean Seamounts." *Marine and Freshwater Research* 59, no. 3 (May 21, 2008): 269–78. doi:10.1071/MFO7131.
- Lorenzen, Kai. "Toward a New Paradigm for Growth Modeling in Fisheries Stock Assessments: Embracing Plasticity and Its Consequences." *Fisheries Research*, Growth: theory, estimation, and application in fishery stock assessment models, 180 (August 2016): 4–22. doi:10.1016/j.fishres.2016.01.006.
- Mangel, Marc, Alec D. MacCall, Jon Brodziak, E.J. Dick, Robyn E. Forrest, Roxanna Pourzand, and Stephen Ralston. "A Perspective on Steepness, Reference Points, and Stock Assessment." *Canadian Journal of Fisheries and Aquatic Sciences* 70, no. 6 (April 9, 2013): 930–40. doi:10.1139/cjfas-2012-0372.
- Maunder, Mark N., and André E. Punt. "A Review of Integrated Analysis in Fisheries Stock Assessment." *Fisheries Research* 142 (May 2013): 61–74. doi:10.1016/j.fishres.2012.07.025.
- Maunder, Mark N., and George M. Watters. "A General Framework for Integrating Environmental Time Series into Stock Assessment Models: Model Description, Simulation Testing, and Example." *Fishery Bulletin* 101, no. 1 (2003): 89–99.
- Methot, Richard D., and Ian G. Taylor. "Adjusting for Bias due to Variability of Estimated Recruitments in Fishery Assessment Models." *Canadian Journal of Fisheries and Aquatic Sciences* 68, no. 10 (October 1, 2011): 1744–60. doi:10.1139/f2011-092.
- Methot, Richard D., and Chantell R. Wetzel. "Stock Synthesis: A Biological and Statistical Framework for Fish Stock Assessment and Fishery Management." *Fisheries Research* 142 (May 2013): 86–99. doi:10.1016/j.fishres.2012.10.012.
- Morrongiello, John R., David A. Crook, Alison J. King, David S. L. Ramsey, and Paul Brown. "Impacts of Drought and Predicted Effects of Climate Change on Fish Growth in Temperate Australian Lakes." *Global Change Biology* 17, no. 2 (February 1, 2011): 745–55. doi:10.1111/j.1365-2486.2010.02259.x.

- Mueter, F. J., N. A. Bond, J. N. Ianelli, and A. B. Hollowed. “Expected Declines in Recruitment of Walleye Pollock (*Theragra Chalcogramma*) in the Eastern Bering Sea under Future Climate Change.” *ICES Journal of Marine Science* 68, no. 6 (July 1, 2011): 1284–96. doi:10.1093/icesjms/fsr022.
- Palmer, M. J., B. F. Phillips, and G. T. Smith. “Application of Nonlinear Models with Random Coefficients to Growth Data.” *Biometrics* 47, no. 2 (1991): 623–35. doi:10.2307/2532151.
- Palumbi, Stephen R. “Fisheries Science: Why Mothers Matter.” *Nature* 430, no. 7000 (August 5, 2004): 621–22. doi:10.1038/430621a.
- Pannella, Georgio. “Growth Patterns in Fish Sagittae.” In *Skeletal Growth of Aquatic Organisms. Biological Records of Environmental Change.*, 519–560. Topics in Geobiology. Springer US, 1980.
- Pikitch, E. K., C. Santora, E. A. Babcock, A. Bakun, R. Bonfil, D. O. Conover, P. Dayton, et al. “Ecosystem-Based Fishery Management.” *Science* 305, no. 5682 (July 16, 2004): 346–47. doi:10.1126/science.1098222.
- Pinheiro, José C., and Douglas M. Bates. “Linear Mixed-Effects Models: Basic Concepts and Examples.” In *Mixed-Effects Models in S and S-PLUS*, 3–56. Statistics and Computing. Springer New York, 2000. doi:10.1007/0-387-22747-4_1.
- Pinsky, Malin L., Boris Worm, Michael J. Fogarty, Jorge L. Sarmiento, and Simon A. Levin. “Marine Taxa Track Local Climate Velocities.” *Science* 341, no. 6151 (September 13, 2013): 1239–42. doi:10.1126/science.1239352.
- Punt, A. E. “Refocusing Stock Assessment in Support of Policy Evaluation.” In *Fisheries for Global Welfare and Environment: Memorial Book of the 5th World Fisheries Congress 2008*, edited by K. Tsukamoto, T. Kawamura, T. Takeuchi, T. D. Beard Jr, and M. J. Kaiser, 139–52, 2008.
https://www.terrapub.co.jp/onlineproceedings/fs/wfc2008/pdf/wfcbk_139.pdf.
- Punt, André E., Teresa A’mar, Nicholas A. Bond, Douglas S. Butterworth, Carryn L. de Moor, José A. A. De Oliveira, Melissa A. Haltuch, Anne B. Hollowed, and Cody Szuwalski. “Fisheries Management under Climate and Environmental Uncertainty: Control Rules and Performance Simulation.” *ICES Journal of Marine Science: Journal Du Conseil* 71, no. 8 (October 1, 2014): 2208–20. doi:10.1093/icesjms/fst057.

- Punt, André E, Doug S Butterworth, Carryn L de Moor, José A A De Oliveira, and Malcolm Haddon. "Management Strategy Evaluation: Best Practices." *Fish and Fisheries* 17, no. 2 (June 1, 2016): 303–34. doi:10.1111/faf.12104.
- Punt, André E., David C. Smith, Kyne KrusicGolub, and Simon Robertson. "Quantifying Age-Reading Error for Use in Fisheries Stock Assessments, with Application to Species in Australia's Southern and Eastern Scalefish and Shark Fishery." *Canadian Journal of Fisheries and Aquatic Sciences* 65, no. 9 (September 1, 2008): 1991–2005. doi:10.1139/F08-111.
- Rahikainen, Mika, and Robert L. Stephenson. "Consequences of Growth Variation in Northern Baltic Herring for Assessment and Management." *ICES Journal of Marine Science* 61, no. 3 (January 1, 2004): 338–50. doi:10.1016/j.icesjms.2004.02.005.
- Redner, Richard A., and Homer F. Walker. "Mixture Densities, Maximum Likelihood and the EM Algorithm." *SIAM Review* 26, no. 2 (1984): 195–239.
- Rosenberg, Andrew A., and Victor R. Restrepo. "Uncertainty and Risk Evaluation in Stock Assessment Advice for U.S. Marine Fisheries." *Canadian Journal of Fisheries and Aquatic Sciences* 51, no. 12 (December 1, 1994): 2715–20. doi:10.1139/f94-271.
- Rowe, Rebecca J., and Rebecca C. Terry. "Small Mammal Responses to Environmental Change: Integrating Past and Present Dynamics." *Journal of Mammalogy* 95, no. 6 (December 1, 2014): 1157–74. doi:10.1644/13-MAMM-S-079.
- Schirripa, Michael J., and J. J. Colbert. "Interannual Changes in Sablefish (*Anoplopoma Fimbria*) Recruitment in Relation to Oceanographic Conditions within the California Current System." *Fisheries Oceanography* 15, no. 1 (January 1, 2006): 25–36. doi:10.1111/j.1365-2419.2005.00352.x.
- Schirripa, Michael J., C. Phillip Goodyear, and Richard M. Methot. "Testing Different Methods of Incorporating Climate Data into the Assessment of US West Coast Sablefish." *ICES Journal of Marine Science: Journal Du Conseil* 66, no. 7 (August 1, 2009): 1605–13. doi:10.1093/icesjms/fsp043.
- Stawitz, Christine C., Timothy E. Essington, Trevor A. Branch, Melissa A. Haltuch, Anne B. Hollowed, and Paul D. Spencer. "A State-Space Approach for Detecting Growth Variation and Application to North Pacific Groundfish." *Canadian*

- Journal of Fisheries and Aquatic Sciences* 72, no. 9 (April 21, 2015): 1316–28. doi:10.1139/cjfas-2014-0558.
- Strom, Are, Robert C. Francis, Nathan J. Mantua, Edward L. Miles, and David L. Peterson. “North Pacific Climate Recorded in Growth Rings of Geoduck Clams: A New Tool for Paleoenvironmental Reconstruction.” *Geophysical Research Letters* 31, no. 6 (2004): L06206. doi:10.1029/2004GL019440.
- Sünksen, Kaj, Claus Stenberg, and Peter Grønkjær. “Temperature Effects on Growth of Juvenile Greenland Halibut (*Reinhardtius Hippoglossoides* Walbaum) in West Greenland Waters.” *Journal of Sea Research*, Proceedings of the Seventh International Symposium on Flatfish Ecology, Part I, 64, no. 1–2 (July 2010): 125–32. doi:10.1016/j.seares.2009.10.006.
- Taylor, Ian G., and Richard D. Methot. “Hiding or Dead? A Computationally Efficient Model of Selective Fisheries Mortality.” *Fisheries Research* 142 (May 2013): 75–85. doi:10.1016/j.fishres.2012.08.021.
- Thorson, James T. “Spatio-Temporal Variation in Fish Condition Is Not Consistently Explained by Density, Temperature, or Season for California Current Groundfishes.” *Marine Ecology Progress Series* 526 (2015): 101–112.
- Thorson, James T., Allan C. Hicks, and Richard D. Methot. “Random Effect Estimation of Time-Varying Factors in Stock Synthesis.” *ICES Journal of Marine Science: Journal Du Conseil* 72, no. 1 (January 1, 2015): 178–85. doi:10.1093/icesjms/fst211.
- Thorson, James T., Olaf P. Jensen, and Elise F. Zipkin. “How Variable Is Recruitment for Exploited Marine Fishes? A Hierarchical Model for Testing Life History Theory.” *Canadian Journal of Fisheries and Aquatic Sciences* 71, no. 7 (March 3, 2014): 973–83. doi:10.1139/cjfas-2013-0645.
- Thorson, James T., and Carolina V. Minte-Vera. “Relative Magnitude of Cohort, Age, and Year Effects on Size at Age of Exploited Marine Fishes.” *Fisheries Research*, Growth: theory, estimation, and application in fishery stock assessment models, 180 (August 2016): 45–53. doi:10.1016/j.fishres.2014.11.016.
- Thorson, James T., Cole C. Monnahan, and Jason M. Cope. “The Potential Impact of Time-Variation in Vital Rates on Fisheries Management Targets for Marine

- Fishes.” *Fisheries Research* 169 (September 2015): 8–17.
doi:10.1016/j.fishres.2015.04.007.
- Thorson, James T., Malin L. Pinsky, and Eric J. Ward. “Model-Based Inference for Estimating Shifts in Species Distribution, Area Occupied and Centre of Gravity.” *Methods in Ecology and Evolution* 7, no. 8 (August 1, 2016): 990–1002.
doi:10.1111/2041-210X.12567.
- Thorson, James T., Ian J. Stewart, Ian G. Taylor, and André E. Punt. “Using a Recruitment-Linked Multispecies Stock Assessment Model to Estimate Common Trends in Recruitment for US West Coast Groundfishes.” *Marine Ecology Progress Series* 483 (May 30, 2013): 245–56. doi:10.3354/meps10295.
- Tolimieri, Nick, and Phillip S. Levin. “The Roles of Fishing and Climate in the Population Dynamics of Bocaccio Rockfish.” *Ecological Applications* 15, no. 2 (April 1, 2005): 458–68.
- Vincenzi, Simone, Alain J. Crivelli, Stephan Munch, Hans J. Skaug, and Marc Mangel. “Trade-Offs between Accuracy and Interpretability in von Bertalanffy Random-Effects Models of Growth.” *Ecological Applications* 26, no. 5 (July 1, 2016): 1535–52. doi:10.1890/15-1177.
- Von Bertalanffy, L. “Quantitative Laws in Metabolism and Growth.” *The Quarterly Review of Biology* 32, no. 3 (September 1957): 217–31.
- Warton, David I., F. Guillaume Blanchet, Robert B. O’Hara, Otso Ovaskainen, Sara Taskinen, Steven C. Walker, and Francis K. C. Hui. “So Many Variables: Joint Modeling in Community Ecology.” *Trends in Ecology & Evolution* 30, no. 12 (December 2015): 766–79. doi:10.1016/j.tree.2015.09.007.
- Weatherley, A. H. “Approaches to Understanding Fish Growth.” *Transactions of the American Fisheries Society* 119, no. 4 (July 1, 1990): 662–72. doi:10.1577/1548-8659(1990)119<0662:ATUFG>2.3.CO;2.
- Webber, D’Arcy N., and James T. Thorson. “Variation in Growth among Individuals and over Time: A Case Study and Simulation Experiment Involving Tagged Antarctic Toothfish.” *Fisheries Research*, Growth: theory, estimation, and application in fishery stock assessment models, 180 (August 2016): 67–76.
doi:10.1016/j.fishres.2015.08.016.

- Weisberg, Sanford, George Spangler, and Laurie S. Richmond. "Mixed Effects Models for Fish Growth." *Canadian Journal of Fisheries and Aquatic Sciences* 67, no. 2 (January 16, 2010): 269–77. doi:10.1139/F09-181.
- Wishart, John. "Growth-Rate Determinations in Nutrition Studies with the Bacon Pig, and Their Analysis." *Biometrika* 30, no. 1/2 (1938): 16–28. doi:10.2307/2332221.
- Xu, Hao, Yujun Sun, Xinjie Wang, Yao Fu, Yunfei Dong, and Ying Li. "Nonlinear Mixed-Effects (NLME) Diameter Growth Models for Individual China-Fir (*Cunninghamia Lanceolata*) Trees in Southeast China." *PLoS ONE* 9, no. 8 (August 1, 2014). doi:10.1371/journal.pone.0104012.
- Zeger, Scott L., and Kung-Yee Liang. "Longitudinal Data Analysis for Discrete and Continuous Outcomes." *Biometrics* 42, no. 1 (1986): 121–30. doi:10.2307/2531248.

APPENDIX A

Supplementary Material for Chapter Two

Supplementary Figures

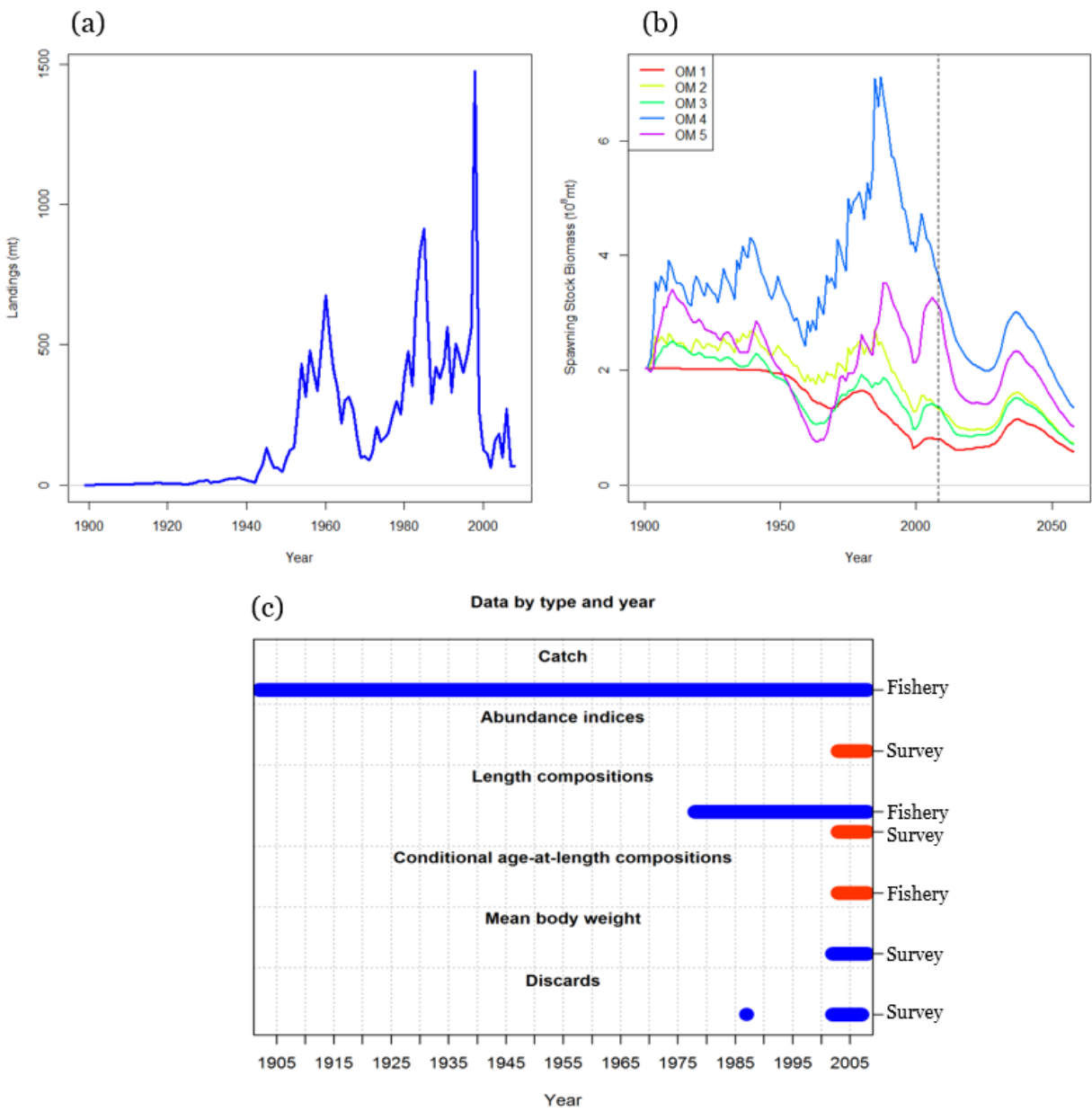


Figure S2.1. (a) Illustration of catch during the historical period for splitnose rockfish (which is used as true catch in the OM), as well as (b) the true spawning biomass trajectory

for a single replicate of the simulation experiment for each OM. (c) Plot showing data types generated in the simulation.

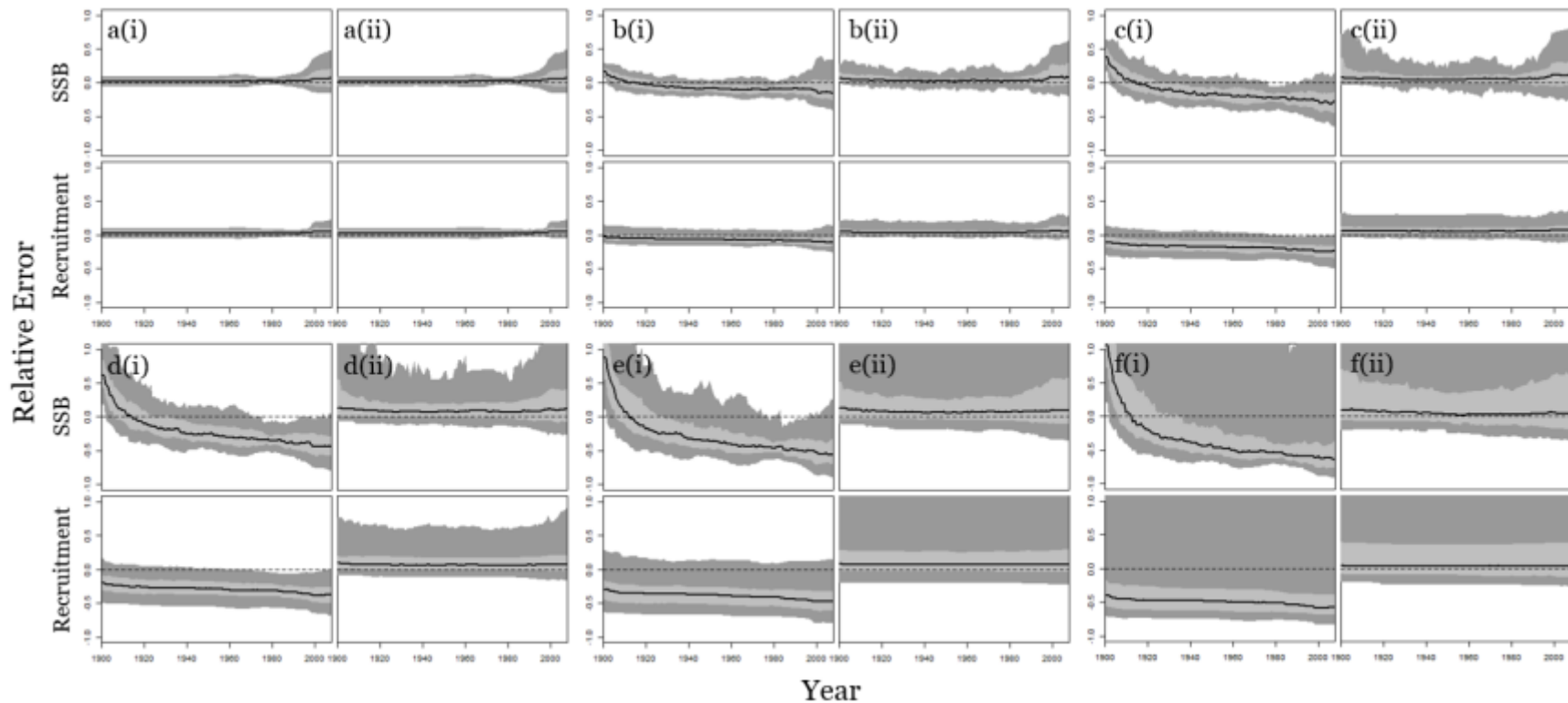


Figure S2.2. Time series of relative errors in estimates of spawning stock biomass (top row of labelled panel) and recruitment (bottom row of labelled panel), showing the results of the sensitivity analysis to the β value. Each letter (a-f) represents an OM with absolute β values ranging from 0 to 0.5 in 0.1 increments, whereas each roman numeral (i-ii) corresponds to an EM (i=growth assumed to be constant; ii=estimating time-varying growth). The black line is the median relative error, the light grey area the 50% simulation intervals, the dark grey area 95% simulation intervals.

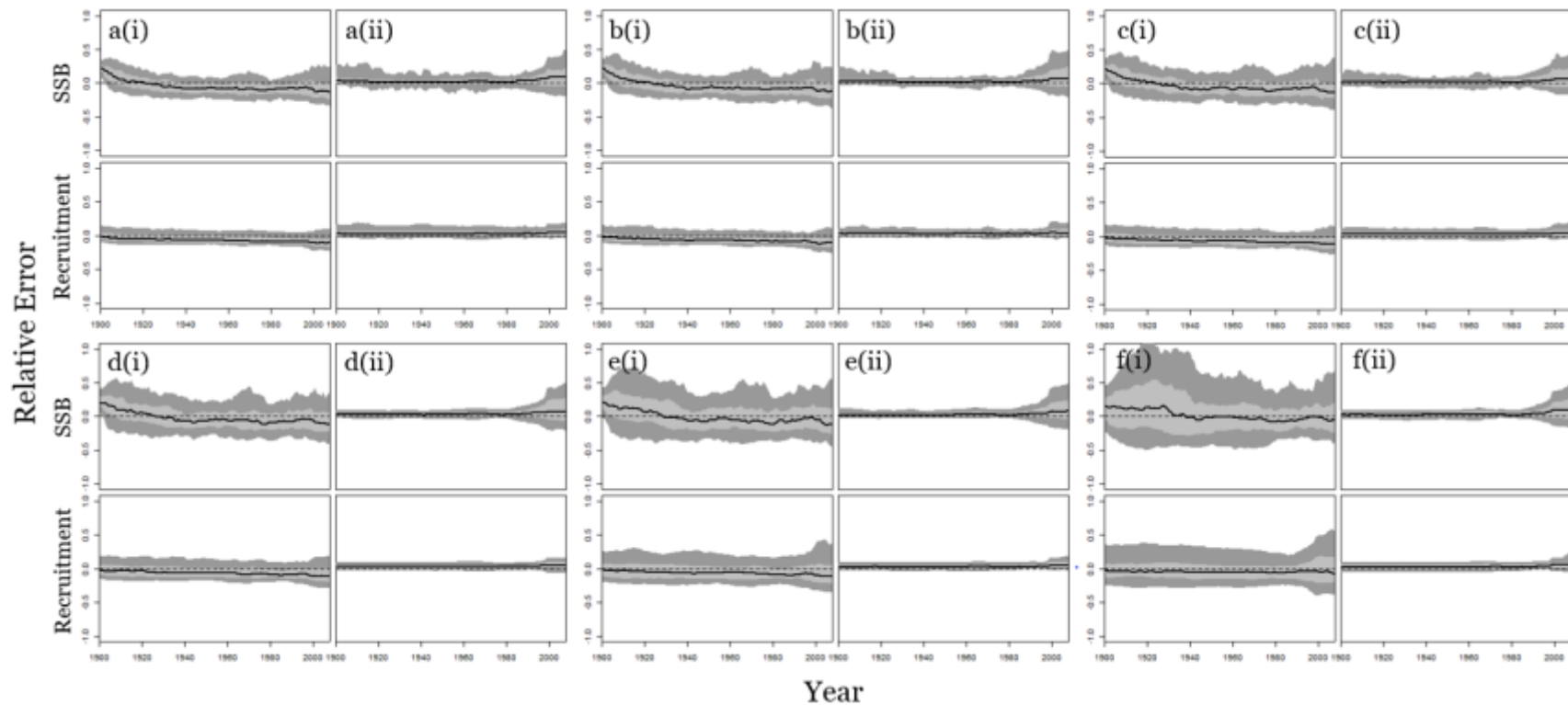


Figure S2.3. Time series of relative errors in estimates of spawning stock biomass (top row of labelled panel) and recruitment (bottom row of labelled panel), showing the results of the sensitivity analysis to the AR ρ value. Each letter (a-f) represents an OM with ρ values ranging from 0 to 0.8 in 0.2 increments, with the final panel showing an OM with ρ value 0.95, whereas each roman numeral (i-ii) corresponds to an EM (i=growth assumed to be constant; ii=estimating time-varying growth). The black line is the median relative error, the light grey area the 50% simulation intervals, the dark grey area 95% simulation intervals.

Supplementary Tables

Table S2.1. Splitnose-rockfish-like parameters Ibid. of the OM and EM and how they were treated in the EM. Estimation of β parameters varied depending on scenario, while the selectivity parameters were either pre-specified or estimated treated equally across scenarios. More details on the parameters and their associated functions are outlined in Methot and Wetzel (2013).

Symbol	Description	True Value		EM treatment
		Female	Male	
Growth and maturity parameters				
M	Natural mortality (yr^{-1})	0.048	0.048	Pre-specified
L_1	Length at age 0 (cm)	9.88	9.88	Estimated
L_2	Asymptotic length (L_∞ [cm] in Eq 1b)	26.6	24.8	Estimated
K	von Bertalanffy growth coefficient (yr^{-1}) (Eq 1b)	0.228	0.25	Estimated
CV_1	Variability in size-at-age for fish less than or equal to L_1	0.0838	0.109	Estimated
CV_2	Variability in size-at-age for fish up to L_2	0.127	0.11	Estimated
β_1	Multiplicative link parameter to L_2	Varies	Varies	Varies
β_2	Multiplicative link parameter to K	Varies	Varies	Varies
Wtlen_1	Weight coefficient (kg cm^{-3})	2.00×10^{-5}	2.00×10^{-5}	Pre-specified
Wtlen_2	Weight exponent	3.014	2.97	Pre-specified
Mat50%	Length at 50% maturity (cm)	21.8		Pre-specified
Mat95%	Length at 95% maturity (cm)	21.9		Pre-specified
Eggs/kg_inter		238000		Pre-specified
Eggs/kg_slope_wt		74300		Pre-specified
Recruitment parameters		<u>Non-sex-specific</u>		
R_o	Initial recruitment (log)	8		Estimated

h	Stock-recruitment steepness	0.58	Pre-specified
σ_R	Recruitment variability	1	Pre-specified
Selectivity parameters			
Fishery φ_1	Peak of double-normal curve (starting length at which selectivity = 1.0) (cm)	33.7	Estimated
Fishery φ_2	Length at which selectivity = 1.0 ends (logistic; cm)	38	Pre-specified
Fishery φ_3	Width of ascending part of curve (exponentiated)	37	Estimated
Fishery φ_4	Width of descending part of curve (exponentiated)	55	Pre-specified
Fishery φ_5	Selectivity at first length bin (logistic)	0.007	Pre-specified
Fishery φ_6	Selectivity at last length bin (logistic)	1.00	Pre-specified
Fishery (retained) φ_1	Inflection of logistic curve	19.9	Estimated
Fishery (retained) φ_2	Slope of curve	2.5	Estimated
Fishery (retained) φ_3	Asymptotic retention	0.99	Estimated
Fishery (retained) φ_4	Slope of curve for males	Same as for females	Pre-specified
Survey φ_1	Starting length at which selectivity = 1.0 (cm)	13.5	Estimated
Survey φ_2	Length at which selectivity = 1.0 ends (logistic; cm)	20.4	Pre-specified
Survey φ_3	Width of ascending part of curve (exponentiated)	7	Estimated
Survey φ_4	Width of descending part of curve (exponentiated)	55	Pre-specified
Survey φ_5	Selectivity at first length bin (logistic)	0.007	Pre-specified
Survey φ_6	Selectivity at last length bin (logistic)	1.00	Pre-specified

Table S2.2. Median relative errors for the parameters and derived quantities.

State of Nature (OM)	Scenario	Parameters												Derived Quantities			
		K_f	K_m	$L_{\infty,f}$	$L_{2,m}$	$\beta_{1,f}$	$\beta_{1,m}$	$\beta_{2,f}$	$\beta_{2,m}$	$CV_{0,f}$	$CV_{0,m}$	$CV_{\infty,f}$	$CV_{\infty,m}$	$\ln R_0$	B_0	B_{2008}	MSY
Not Climate-Driven	1-0-A	0.00	0.00	0.00	0.00	NA	NA	NA	NA	0.00	0.00	0.01	0.01	0.00	0.01	0.06	0.02
	1-0-B	0.00	0.00	0.00	0.00	0.00	0.00	0.00	0.00	0.00	0.00	0.01	0.01	0.00	0.01	0.06	0.02
Weakly Climate-Driven	2-0-A	-0.20	-0.19	0.07	0.05	NA	NA	NA	NA	0.01	-0.02	0.06	0.05	0.00	0.21	-0.12	0.05
	2-1-B	-0.02	-0.02	0.00	0.00	-0.22	-0.11	-0.08	-0.1	-0.01	0.00	0.02	0.02	0.00	0.05	0.09	0.04
	2-2-B	-0.17	-0.16	0.05	0.04	-0.91	-0.37	-0.54	-0.49	-0.02	-0.02	0.06	0.04	0.00	0.20	-0.02	0.08
	2-3-B	-0.08	-0.06	0.02	0.01	-1.42	-1.11	-1.33	-1.41	0.00	0.00	0.03	0.02	0.00	0.15	0.08	0.05
	2-4-B	-0.11	-0.08	0.04	0.02	0.22	-0.49	-0.33	-0.58	0.01	0.00	0.03	0.02	0.00	0.17	0.07	0.06
Climate-Driven (High AR)	3-0-A	-0.13	-0.14	0.05	0.04	NA	NA	NA	NA	0.00	-0.03	0.05	0.04	0.00	0.14	-0.05	0.02
	3-1-B	0.00	0.00	0.00	0.00	-0.06	-0.01	-0.02	-0.02	0.00	0.00	0.01	0.01	0.00	0.02	0.09	0.03
Climate-Driven (High Beta)	4-0-A	-0.51	-0.56	0.28	0.31	NA	NA	NA	NA	0.13	0.03	0.23	0.22	-0.03	0.61	-0.44	0.10
	4-1-B	-0.01	-0.02	0.00	0.00	-0.05	-0.06	-0.02	-0.02	0.00	0.00	0.02	0.02	0.01	0.13	0.12	0.12
Climate-Driven (High AR and High Beta)	5-0-A	-0.38	-0.44	0.21	0.23	NA	NA	NA	NA	0.04	0.00	0.23	0.23	-0.01	0.14	-0.24	0.03
	5-1-B	0.00	0.00	0.00	0.00	-0.01	-0.05	-0.01	-0.01	-0.01	0.00	0.01	0.01	0.00	0.02	0.07	0.02
	5-2-B	-0.38	-0.43	0.15	0.17	-0.27	-0.46	-0.23	-0.21	0.03	-0.02	0.13	0.11	0.00	0.52	-0.03	0.21
	5-3-B	-0.37	-0.40	0.26	0.30	-1.07	-1.02	-1.05	-1.16	0.05	-0.01	0.09	0.06	0.00	0.67	-0.23	0.26
	5-4-B	-0.20	-0.22	0.10	0.12	-1.05	-1.03	-0.98	-0.97	0.05	0.00	0.07	0.08	0.01	0.07	0.15	-0.07

Table S2.3. Size-at-age for the first forty years of the OM for a single replicate for OM 5. Each cell is coloured from red to green as their value increases, and cells where size-at-age is identical to the preceding age in the preceding year (i.e., because Stock Synthesis does not allow fish to shrink) after the environmental index begins (1901) are outlined.

Yr	Age																																													
	0	1	2	3	4	5	6	7	8	9	10	11	12	13	14	15	16	17	18	19	20	21	22	23	24	25	26	27	28	29	30	31	32	33	34	35	36	37	38	39	40					
1900	2	6.74044	11.0589	14.2712	16.7753	19.7439	20.3561	21.6199	22.6259	23.4247	24.0444	24.5721	24.9763	25.2911	25.5543	25.7592	25.9206	26.0499	26.1528	26.2348	26.3	26.3519	26.3933	26.4262	26.4524	26.4733	26.4899	26.5031	26.5124	26.522	26.5237	26.524	26.5332	26.5416	26.5443	26.5464	26.5481	26.5495	26.5504	26.5514	26.5521					
1901	2	6.74044	11.0637	14.2712	16.7753	19.7439	20.3561	21.6199	22.6259	23.4247	24.0444	24.5721	24.9763	25.2911	25.5543	25.7592	25.9206	26.0499	26.1528	26.2348	26.3	26.3519	26.3933	26.4262	26.4524	26.4733	26.4899	26.5031	26.5124	26.522	26.5237	26.524	26.5332	26.5416	26.5443	26.5464	26.5481	26.5495	26.5504	26.5514	26.5521					
1902	2	6.74044	11.0649	14.0164	16.5241	19.4819	20.4006	21.2015	22.2645	23.056	23.6322	24.1009	24.5715	24.9763	25.2911	25.5543	25.7592	25.9206	26.0499	26.1528	26.2348	26.3	26.3519	26.3933	26.4262	26.4524	26.4733	26.4899	26.5031	26.5124	26.522	26.5237	26.524	26.5332	26.5416	26.5443	26.5464	26.5481	26.5495	26.5504	26.5514	26.5521				
1903	2	6.74044	11.2001	14.350	16.6565	19.6452	20.2324	21.492	22.476	23.2673	23.9974	24.399	24.7903	25.152	25.4355	25.6933	25.9385	26.0610	26.1619	26.2495	26.3279	26.4043	26.4795	26.5534	26.5705	26.5964	26.6179	26.6346	26.6479	26.6595	26.667	26.6737	26.679	26.6833	26.6867	26.6894	26.6915	26.6932	26.6946	26.6957	26.6965					
1904	2	6.74044	11.2282	14.9199	17.4018	19.395	21.0669	22.3722	23.4114	24.2338	24.9975	25.4219	25.8394	26.1710	26.4356	26.7022	26.9167	27.0875	27.2235	27.3310	27.418	27.4864	27.5412	27.5847	27.6193	27.6469	27.6663	27.7003	27.7113	27.7201	27.7272	27.7326	27.7372	27.7400	27.7426	27.7458	27.7476	27.749	27.7502	27.7511						
1905	2	6.74044	11.2516	14.6933	17.7242	19.8271	21.3959	22.767	23.9374	24.8396	25.3681	25.9053	26.3303	26.6907	26.9533	27.1696	27.3382	27.5641	27.7042	27.8157	27.9045	27.9752	28.0315	28.0763	28.1119	28.1403	28.1629	28.1809	28.1953	28.2067	28.2159	28.223	28.2287	28.2333	28.237	28.2399	28.2422	28.244	28.2455	28.2467	28.2476					
1906	2	6.74044	11.2689	14.7979	17.4439	20.4432	21.9774	23.1728	24.3040	25.1834	25.592	26.4521	26.9901	27.2531	27.5357	27.7609	27.9394	28.1190	28.2651	28.3807	28.4728	28.5461	28.6044	28.6509	28.6879	28.7173	28.7400	28.7594	28.7743	28.7851	28.7955	28.803	28.809	28.8138	28.8176	28.8206	28.823	28.8249	28.8264	28.8276	28.8286					
1907	2	6.74044	11.1997	14.8713	17.7993	20.1605	22.234	23.473	24.7475	25.6364	26.199	27.0035	27.4682	27.8332	28.1527	28.3672	28.5539	28.7021	28.8518	28.9723	29.0653	29.1447	29.2055	29.2539	29.2924	29.3231	29.3475	29.367	29.3825	29.3949	29.4046	29.4124	29.4197	29.4226	29.4275	29.4307	29.4332	29.4358	29.4381	29.439						
1908	2	6.74044	11.2599	14.5704	17.5647	19.9661	21.9666	23.593	24.7223	25.5973	26.3411	26.9574	27.4321	27.8191	28.11	28.2506	28.5413	28.6932	28.937	29.2584	29.3235	29.3815	29.4276	29.4623	29.4869	29.5092	29.5292	29.547	29.5634	29.5781	29.5914	29.6034	29.6143	29.6241	29.6329	29.6404	29.6472	29.6531	29.6581	29.6621	29.6661					
1909	2	6.74044	11.2559	14.9323	17.5795	20.0501	22.0215	23.6197	25.0063	25.9749	26.6961	27.3301	27.8226	28.2165	28.5292	28.7762	28.9765	29.1243	29.26	29.3597	29.4605	29.546	29.6062	29.6575	29.6993	29.7304	29.7564	29.7804	29.8008	29.8172	29.8301	29.8404	29.8486	29.8551	29.8603	29.8644	29.8677	29.8702	29.8723	29.874	29.8753					
1910	2	6.74044	11.1175	14.816	17.7731	20.043	22.0857	23.7146	25.0242	26.1819	26.9923	27.5801	28.1026	28.5905	28.9352	29.0927	29.2995	29.4634	29.5939	29.6977	29.7802	29.8435	29.9305	29.9839	30.0263	30.06	30.0845	30.1002	30.1279	30.1448	30.1593	30.1643	30.1696	30.1929	30.1973	30.2	30.2022	30.2039	30.2053							
1911	2	6.74044	11.1462	14.4602	17.4004	19.7859	21.6172	23.2165	24.5791	25.6388	26.5495	27.2152	27.6976	28.1197	28.5105	28.8352	29.0927	29.2995	29.4634	29.5939	29.6977	29.7802	29.8435	29.9305	29.9839	30.0263	30.06	30.0845	30.1002	30.1279	30.1448	30.1593	30.1643	30.1696	30.1929	30.1973	30.2	30.2022	30.2039							
1912	2	6.74044	11.1726	14.355	17.009	19.3626	21.274	22.7405	24.0402	25.1126	26.0613	26.7045	27.2227	27.6976	28.1197	28.5105	28.8352	29.0927	29.2995	29.4634	29.5939	29.6977	29.7802	29.8435	29.9305	29.9839	30.0263	30.06	30.0845	30.1002	30.1279	30.1448	30.1593	30.1643	30.1696	30.1929	30.1973	30.2	30.2022							
1913	2	6.74044	11.1991	14.4694	17.0375	19.1799	21.0066	22.6228	23.9664	24.9719	25.7214	26.4065	27.0001	27.4448	27.8505	28.2352	28.5997	29.2995	29.4634	29.5939	29.6977	29.7802	29.8435	29.9305	29.9839	30.0263	30.06	30.0845	30.1002	30.1279	30.1448	30.1593	30.1643	30.1696	30.1929	30.1973	30.2									
1914	2	6.74044	11.1417	14.5241	17.1939	19.2763	21.0135	22.5547	23.8052	24.7651	25.6239	26.3177	26.8732	27.3611	27.6999	28.0097	28.2853	28.5792	28.8415	29.0927	29.2995	29.4634	29.5939	29.6977	29.7802	29.8435	29.9305	29.9839	30.0263	30.06	30.0845	30.1002	30.1279	30.1448	30.1593	30.1643	30.1696	30.1929	30.1973							
1915	2	6.74044	11.0516	14.3364	17.4947	19.177	21.0425	22.2319	23.4646	24.4647	25.2324	25.9233	26.4743	26.9115	27.3411	27.6999	28.0097	28.2853	28.5792	28.8415	29.0927	29.2995	29.4634	29.5939	29.6977	29.7802	29.8435	29.9305	29.9839	30.0263	30.06	30.0845	30.1002	30.1279	30.1448	30.1593	30.1643	30.1696	30.1929	30.1973						
1916	2	6.74044	11.0625	13.9674	16.5235	18.6404	20.2977	21.5953	22.7777	23.631	24.4647	25.2324	25.9233	26.4743	26.9115	27.3411	27.6999	28.0097	28.2853	28.5792	28.8415	29.0927	29.2995	29.4634	29.5939	29.6977	29.7802	29.8435	29.9305	29.9839	30.0263	30.06	30.0845	30.1002	30.1279	30.1448	30.1593	30.1643	30.1696	30.1929	30.1973					
1917	2	6.74044	11.1104	13.7071	16.1444	18.1241	19.7594	21.0415	22.0452	22.8924	23.6371	24.4647	25.2324	25.9233	26.4743	26.9115	27.3411	27.6999	28.0097	28.2853	28.5792	28.8415	29.0927	29.2995	29.4634	29.5939	29.6977	29.7802	29.8435	29.9305	29.9839	30.0263	30.06	30.0845	30.1002	30.1279	30.1448	30.1593	30.1643	30.1696	30.1929	30.1973				
1918	2	6.74044	11.1048	14.2075	16.3947	18.1973	19.7644	21.0624	22.0786	22.8741	23.5378	24.1559	24.7917	25.4002	25.9476	26.4743	26.9115	27.3411	27.6999	28.0097	28.2853	28.5792	28.8415	29.0927	29.2995	29.4634	29.5939	29.6977	29.7802	29.8435	29.9305	29.9839	30.0263	30.06	30.0845	30.1002	30.1279	30.1448	30.1593	30.1643	30.1696	30.1929	30.1973			
1919	2	6.74044	11.1937	14.5162	16.9442	19.7355	20.1953	21.466	22.5156	23.3386	23.9829	24.5204	25.0047	25.5385	26.0236	26.472	26.9984	27.5312	27.6166	27.8903	28.142	28.3452	28.6031	28.8415	29.0927	29.2995	29.4634	29.5939	29.6977	29.7802	29.8435	29.9305	29.9839	30.0263	30.06	30.0845	30.1002	30.1279	30.1448	30.1593	30.1643	30.1696	30.1929	30.1973		
1920	2	6.74044	11.0983	14.5534	17.251	19.2386	20.6760	21.842	22.9338	23.746	24.4142	24.9372	25.3737	25.7664	26.1992	26.5983	26.9593	27.3046	27.5967	27.8177	28.1098	28.3142	28.4954	28.6866	28.8821	29.0924	29.2995	29.4634	29.5939	29.6977	29.7802	29.8435	29.9305	29.9839	30.0263	30.06	30.0845	30.1002	30.1279	30.1448	30.1593	30.1643	30.1696	30.1929	30.1973	
1921	2	6.74044	11.0565	14.1597	16.8385	19.1093	20.5993	21.7253	22.6615	23.4765	24.1497	24.6774	25.0907	25.4354	25.7647	26.1982	26.5983	26.9593	27.3046	27.5967	27.8177	28.1098	28.3142	28.4954	28.6866	28.8821	29.0924	29.2995	29.4634	29.5939	29.6977	29.7802	29.8435	29.9305	29.9839	30.0263	30.06	30.0845	30.1002	30.1279	30.1448	30.1593	30.1643	30.1696	30.1929	30.1973
1922	2	6.74044	11.1177	13.9372	16.4044	18.5733	20.1999	21.4246	22.3109	23.6772	24.2024	24.6774	25.0907	25.4354	25.7647	26.1982	26.5983	26.9593	27.3046	27.5967	27.8177	28.1098	28.3142	28.4954	28.6866	28.8821	29.0924	29.2995	29.4634	29.5939	29.6977	29.7802	29.8435	29.9305	29.9839	30.0263	30.06	30.0845	30.1002	30.1279	30.1448	30.1593	30.1643	30.1696	30.1929	30.1973
1923	2	6.74044	11.1359	14.2376	16.5167	18.4397	20.1306	21.451	22.4029	23.1279	23.706	24.213	24.6302	25.0075	25.3357	25.6095	25.8726	26.1449	26.5903	26.9593	27.3046	27.5967	27.8177																							

Table S2.4. Summary table showing results of index misspecification.

State of Nature (OM)	Observation Model	Performance Metric		
	Index Accuracy (α value)	Relative Lost Yield (Interquartile Range)	Est B2058/ True B2058 (Interquartile Range)	Proportion of Replicates Overfished
Climate-Driven (High AR and High Beta)	NA	-0.0308 (0.758)	1 (0.555)	0.42
	1	0.0217 (0.1)	0.985 (0.105)	0.45
	0.8	0.0568 (0.429)	0.986 (0.57)	0.5
	0.6	0.0625 (0.589)	0.97 (0.641)	0.5
	0.4	0.0716 (0.696)	1 (0.557)	0.5
	0.2	-0.0343 (0.782)	1 (0.8)	0.48
	0	0.206 (1.57)	1 (0.844)	0.5